The Astronomical Journal, 135:1766–1784, 2008 May doi:10.1088/0004-6256/135/5/1766

FIRST-YEAR SPECTROSCOPY FOR THE SLOAN DIGITAL SKY SURVEY-II SUPERNOVA SURVEY

Chen Zheng[1], Roger W. Romani[1], Masao Sako[2], John Marriner[3], Bruce Bassett[4,5], Andrew Becker[6], Changsu Choi[7], David Cinabro[8], Fritz DeJongh[3], Darren L. Depoy[9], Ben Dilday[10,11], Mamoru Doi[12], Joshua A. Frieman[3,11,13], Peter M. Garnavich[14], Craig J. Hogan[6], Jon Holtzman[15], Myungshin Im[7], Saurabh Jha[1], Richard Kessler[11,16], Kohki Konishi[17], Hubert Lampeitl[18], Jennifer L. Marshall[9], David McGinnis[3], Gajus Miknaitis[3], Robert C. Nichol[19], Jose Luis Prieto[9], Adam G. Riess[18,20], Michael W. Richmond[21], Donald P. Schneider[22], Mathew Smith[19], Naohiro Takanashi[12], Kouichi Tokita[12], Kurt van der Heyden[5], Naoki Yasuda[17], Roberto J. Assef[9], John Barentine[23,24], Ralf Bender[25,26], Roger D. Blandford[1], Malcolm Bremer[27], Howard Brewington[24], Chris A. Collins[28], Arlin Crotts[29], Jack Dembicky[24], Jason Eastman[9], Alastair Edge[30], Ed Elson[4,5], Michael E. Eyler[31], Alexei V. Filippenko[32], Ryan J. Foley[32], Stephan Frank[9], Ariel Goobar[33], Michael Harvanek[24,34], Ulrich Hopp[25,26], Yutaka Ihara[12], Steven Kahn[1], William Ketzeback[24], Scott J. Kleinman[24,35], Wolfram Kollatschny[36], Jurek Krzesiński[24,37], Giorgos Leloudas[38], Daniel C. Long[24], John Lucey[30], Elena Malanushenko[24], Viktor Malanushenko[24], Russet J. McMillan[24], Christopher W. Morgan[9,31], Tomoki Morokuma[12,39], Atsuko Nitta[24,40], Linda Ostman[33], Kaike Pan[24], A. Kathy Romer[41], Gabrelle Saurage[24], Katie Schlesinger[9], Stephanie A. Snedden[24], Jesper Sollerman[38,42], Maximilian Stritzinger[38], Linda C. Watson[9], Shannon Watters[24], J. Craig Wheeler[23], and Donald York[13,16]

[1] Kavli Institute for Particle Astrophysics and Cosmology, Stanford University, Stanford, CA 94305-4060, USA
[2] Department of Physics and Astronomy, University of Pennsylvania, 209 South 33rd Street, Philadelphia, PA 19104, USA
[3] Center for Particle Astrophysics, Fermi National Accelerator Laboratory, P.O. Box 500, Batavia, IL 60510, USA
[4] Department of Mathematics and Applied Mathematics, University of Cape Town, Rondebosch 7701, South Africa
[5] South African Astronomical Observatory, P.O. Box 9, Observatory 7935, South Africa
[6] Department of Astronomy, University of Washington, Box 351580, Seattle, WA 98195, USA
[7] Department of Physics & Astronomy, FPRD, Seoul National University, Seoul, South Korea
[8] Department of Physics, Wayne State University, Detroit, MI 48202, USA
[9] Department of Astronomy, Ohio State University, 140 West 18th Avenue, Columbus, OH 43210-1173, USA
[10] Department of Physics, University of Chicago, Chicago, IL 60637, USA
[11] Kavli Institute for Cosmological Physics, The University of Chicago, 5640 South Ellis Avenue Chicago, IL 60637, USA
[12] Institute of Astronomy, Graduate School of Science, University of Tokyo 2-21-1, Osawa, Mitaka, Tokyo 181-0015, Japan
[13] Department of Astronomy and Astrophysics, The University of Chicago, 5640 South Ellis Avenue, Chicago, IL 60637, USA
[14] University of Notre Dame, 225 Nieuwland Science, Notre Dame, IN 46556-5670, USA
[15] Department of Astronomy, MSC 4500, New Mexico State University, P.O. Box 30001, Las Cruces, NM 88003, USA
[16] Enrico Fermi Institute, University of Chicago, 5640 South Ellis Avenue, Chicago, IL 60637, USA
[17] Institute for Cosmic Ray Research, University of Tokyo, 5-1-5, Kashiwanoha, Kashiwa, Chiba, 277-8582, Japan
[18] Space Telescope Science Institute, 3700 San Martin Drive, Baltimore, MD 21218, USA
[19] Institute of Cosmology and Gravitation, Mercantile House, Hampshire Terrace, University of Portsmouth, Portsmouth PO1 2EG, UK
[20] Department of Physics and Astronomy, Johns Hopkins University, 3400 North Charles Street, Baltimore, MD 21218, USA
[21] Physics Department, Rochester Institute of Technology, 85 Lomb Memorial Drive, Rochester, NY 14623-5603, USA
[22] Department of Astronomy and Astrophysics, The Pennsylvania State University, 525 Davey Laboratory, University Park, PA 16802, USA
[23] Department of Astronomy, McDonald Observatory, University of Texas, Austin, TX 78712, USA
[24] Apache Point Observatory, P.O. Box 59, Sunspot, NM 88349, USA
[25] Universitaets-Sternwarte Munich, 1 Scheinerstr, Munich, D-81679, Germany
[26] Max Planck Institute for Extraterrestrial Physics, D-85748, Garching, Munich, Germany
[27] H. H. Wills Physics Laboratory, University of Bristol, Bristol, BS8 1TL, UK
[28] Astrophysics Research Institute, Liverpool John Moores University, Birkenhead CH41 1LD, UK
[29] Department of Astronomy, Columbia University, New York, NY 10027, USA
[30] Department of Physics, University of Durham, South Road, Durham, DH1 3LE, UK
[31] Department of Physics, United States Naval Academy, 572C Holloway Road, Annapolis, MD 21402, USA
[32] Department of Astronomy, University of California, Berkeley, CA 94720-3411, USA
[33] Physics Department, Stockholm University, AlbaNova University Center, 106 91 Stockholm, Sweden
[34] Lowell Observatory, 1400 Mars Hill Rd., Flagstaff, AZ 86001, USA
[35] Subaru Telescope, 650 N. A'Ohoku Place, Hilo, HI 96720, USA
[36] Institut für Astrophysik, Universität Göttingen, Friedrich-Hund-Platz 1, D-37077 Göttingen, Germany
[37] Obserwatorium Astronomiczne na Suhorze, Akademia Pedagogicazna w Krakowie, ulica Podchorążych 2, PL-30-084 Kraków, Poland
[38] Dark Cosmology Centre, Niels Bohr Institute, University of Copenhagen, DK-2100, Denmark
[39] National Astronomical Observatory of Japan, 2-21-1, Osawa, Mitaka, Tokyo 181-8588, Japan
[40] Gemini Observatory, 670 North A'ohoku Place, Hilo, HI 96720, USA
[41] Astronomy Center, University of Sussex, Falmer, Brighton BN1 9QJ, UK
[42] Astronomy Department, Stockholm University, AlbaNova University Center, 106 91 Stockholm, Sweden
Received 2007 October 28; accepted 2008 February 18; published 2008 April 7

ABSTRACT

This paper presents spectroscopy of supernovae (SNe) discovered in the first season of the Sloan Digital Sky Survey-II SN Survey. This program searches for and measures multi-band light curves of SNe in the redshift range $z = 0.05$–0.4, complementing existing surveys at lower and higher redshifts. Our goal is to better characterize the SN population, with a particular focus on SNe Ia, improving their utility as cosmological distance indicators and as probes of dark energy. Our SN spectroscopy program features rapid-response observations using telescopes of a range of apertures, and provides confirmation of the SN and host-galaxy types as well as precise redshifts.

We describe here the target identification and prioritization, data reduction, redshift measurement, and classification of 129 SNe Ia, 16 spectroscopically probable SNe Ia, 7 SNe Ib/c, and 11 SNe II from the first season. We also describe our efforts to measure and remove the substantial host-galaxy contamination existing in the majority of our SN spectra.

Key words: cosmology: observations – methods: data analysis – supernovae: general – surveys – techniques: spectroscopic

Online-only material: color figures

1. INTRODUCTION

During the last few decades, studies of Type Ia supernovae (SNe Ia) have made significant contributions to our understanding of cosmology. In particular, SN Ia samples from low redshifts ($z \lesssim 0.1$) have helped to constrain the Hubble constant (Hamuy et al. 1996; Jha et al. 1999, 2007). Their comparison with SN Ia samples from high redshifts ($z \gtrsim 0.4$) has led to evidence for an accelerating universe (Riess et al. 1998; Perlmutter et al. 1999; see Filippenko 2005b for a review). The key is that these SNe prove to be remarkably homogeneous "standard candles" after correcting for the empirical luminosity versus decline-rate relation (e.g., Phillips 1993). However, surveys covering large areas with intermediate depth have proved difficult to perform, leading to a "redshift desert" ($0.1 \lesssim z \lesssim 0.4$; Riess et al. 2004) in the SN Ia Hubble diagram. Further, merging data from multiple surveys raises questions of systematics control; high-precision cross calibration is required to differentiate between cosmological models. To further calibrate the SN luminosities, to probe for possible redshift evolution, and to study the empirical properties of the "dark energy" that has been invoked to account for the acceleration of the universe, it is critical to fill in this redshift desert with well-studied data and to connect the low-z and high-z populations.

The SN survey of the Sloan Digital Sky Survey-II (SDSS-II), comprising three three-month campaigns (2005 September through 2007 November), was launched to discover SNe Ia and acquired photometric and spectroscopic observations in this sparsely sampled intermediate-redshift interval of $z = 0.05$–0.4 (Frieman et al. 2007). The large (300 deg^2), moderately deep ($r \approx 22.5$ mag) survey provides a significant volume for untargeted discovery of these intermediate-redshift SNe, thus complementing ongoing low-z surveys and follow-up programs (e.g., Lick Observatory SN Search (LOSS),[43] Li et al. 2000; Filippenko et al. 2001; Filippenko 2005a; Carnegie SN Program (CSP),[44] Hamuy et al. 2006; Nearby SN Factory (SNFactory),[45] Copin et al. 2006; the Center for Astrophysics follow-up effort (CfA) SN Group,[46] Riess et al. 1995, 1999; Riess 1996; Jha et al. 2006, 2007). The survey is sufficiently deep to overlap with the high-z samples (e.g., Canada–France–Hawaii Telescope SN Legacy Survey (SNLS),[47] Astier et al. 2006; Equation of State: SNe trace Cosmic Expansion (ESSENCE),[48] Miknaitis et al. 2007; Wood-Vasey et al. 2007) and help to explore the kinematics of the expanding universe during the interval when most models of dark energy anticipate maximum departure from a simple, flat, Λ-Cold Dark Matter (LCDM) cosmology. The uniformity of the SDSS photometric calibration system provides precise measurements of SN light curves in five filters (*ugriz*; Fukugita et al. 1996). The large survey volume also facilitates discovery of rare SN types, sampling the full extent of the SN Ia population, as well as allowing searches for SNe Ib/c, SNe II, hypernovae, and other peculiar denizens of the astronomical zoo.

This paper describes our spectroscopic follow-up techniques and presents results from spectroscopic observations of SNe discovered in the first season of the SDSS-II SN Survey. During the Fall 2005 campaign, we repeatedly scanned SDSS stripe 82, with alternate observations of the northern and southern strips, maintaining full coverage of the 2.5° wide stripe on a cadence of ∼2 d. SN candidates were identified by rapid on-mountain processing in the g, r, and i filters. Targets that passed a variety of quality control cuts were then inspected by humans and prioritized for spectroscopic follow-up observations (Sako et al. 2007). The primary spectroscopic facilities used to complement the imaging survey were the 2.4 m Hiltner telescope at MDM, the 3.5 m Astronomy Research Consortium (ARC) telescope at Apache Point Observatory (APO), and the queue-scheduled 9.2 m Hobby–Eberly Telescope (HET) at McDonald Observatory. Individual observing campaigns were also conducted with the 4.2 m William Herschel Telescope (WHT), the 8.2 m Subaru, and the 10 m Keck I telescope. A total of 259 spectra were obtained during the first season, yielding 129 spectroscopically confirmed SNe Ia with a wide range of epochs (−12 d to 54 d relative to B-band maximum light), 16 spectroscopically probable SNe Ia, and a handful of other SN types, including peculiar SNe Ia and broad-lined SN Ib/c "hypernovae." Several objects were observed at multiple epochs.

In this paper, we present our spectroscopic data reduction and analysis methods. We briefly summarize the candidate identification and prioritization algorithms (Section 2), and we describe the spectroscopic observations at several follow-up telescopes as well as the basic data reduction (Section 3). In Section 4, we describe the procedures used for SN classification and redshift determination, including efforts to measure and remove spectral contamination by the host-galaxy light. Section 5 summarizes the basic results, describing a few of the peculiar spectra. A complete analysis of the spectral features in the SN Ia population and extension of the analysis to Seasons 2 and 3 are deferred to later publications. However, in Section 6, we note potential results from the analysis of the full spectroscopy data and summarize our present conclusions.

2. SELECTION OF SUPERNOVA CANDIDATES FOR SPECTROSCOPY

The SDSS-II SN Program uses a CCD camera (Gunn et al. 1998) mounted on the APO 2.5 m telescope (Gunn et al. 2006) to obtain repeated scans of a 300 deg^2 region aligned along the

[43] http://astro.berkeley.edu/∼bait/kait.html.
[44] http://csp1.lco.cl/∼cspuser1/PUB/CSP.html.
[45] http://snfactory.lbl.gov/.
[46] http://www.cfa.harvard.edu/cfa/oir/Research/supernova/SNgroup.html.
[47] http://www.cfht.hawaii.edu/SNLS.
[48] http://www.ctio.noao.edu/essence.

celestial equator in the Southern Galactic Hemisphere. Images in this 2.5° × 120° area (SDSS Stripe 82) are obtained almost simultaneously using five filters ($ugriz$; Fukugita et al. 1996). The images have sufficient sensitivity to discover SNe Ia out to $z \approx 0.4$, while providing high-quality light curves (J. Holtzman et al. 2007, in preparation) for a large fraction of the SNe on an accurately calibrated photometric system (∼1%; Ivezic et al. 2007). Technical summaries of the SDSS and the data products can be found in York et al. (2000), Adelman-McCarthy et al. (2007), and references therein. An overview of the SDSS-II SN program is presented by Frieman et al. (2007).

With the large data volume produced for each clear night, it was necessary to flag SN candidates using a dedicated computer cluster at APO. Co-added template images from previous years were registered and convolved to match the search images in the g, r, and i bands. Statistically significant variable sources appearing in two or more filters were flagged. Within 24 h, thousands of new detections from each night of observation were transferred to Fermilab and entered into the SN database. These detections (or "objects") were visually inspected to identify possible SN candidates. Host-galaxy properties (morphology, color, and photometric redshift) were assembled along with estimates for the SN photometric redshift, extinction, date of maximum light, photometric type, and stretch factor, as obtained from the preliminary photometry. For all active candidates, these parameters were updated daily. Visual grading of the candidates produced a cleaner SN set. Efficiencies for selecting true SNe were actively monitored with a large number of "fake" SNe added to the data stream. Details of the candidate identification and characterization are described by Sako et al. (2007).

With such a large number of candidate SNe and limited spectroscopic resources, only the "best" objects were subject to follow-up spectroscopic observations. In particular, during the first season, we focused (with a few exceptions) on objects for which a classification of SN Ia was strongly preferred by the initial photometry. We also selected for large SN–galaxy separation, minimal photometric evidence for dust extinction, and interesting SNe (those with lowest or highest redshift, underluminous hosts, and peculiar light curves). This approach certainly biases the distribution of SN properties, except for $z \lesssim 0.12$, where we attempted to make the data as complete as possible (Dilday et al. 2008). These "best" SNe were assigned to the various telescopes: APO, MDM, and WHT for the brighter objects with lower-estimated redshifts, or HET and Subaru for the fainter distant objects. Significant efforts were made to avoid duplicate observations and to maximize the observation efficiency of each telescope. Only a modest fraction (∼25%) of the selected candidates were not observed within 20 rest-frame days of SN maximum or yielded noisy spectra; host-galaxy spectra and redshifts are being measured for a sample of those objects missed due to poor weather or oversubscribed spectroscopic resources.

3. OBSERVATIONS AND REDUCTIONS

During fall 2005, three telescopes were routinely available for SDSS-II SN spectroscopy: MDM 2.4 m (49 shared nights), ARC 3.5 m (31 half-nights), and HET 9.2 m (64.5 h of queue time). Several additional dedicated campaigns helped greatly, with six nights on the 4.2 m WHT, six shared nights on Subaru, and one target-of-opportunity night on Keck. A handful of additional spectra were obtained at other facilities based on the SDSS-II SN candidate announcements. In total, 259 useful spectra were obtained which yielded 129 spectroscopically confirmed

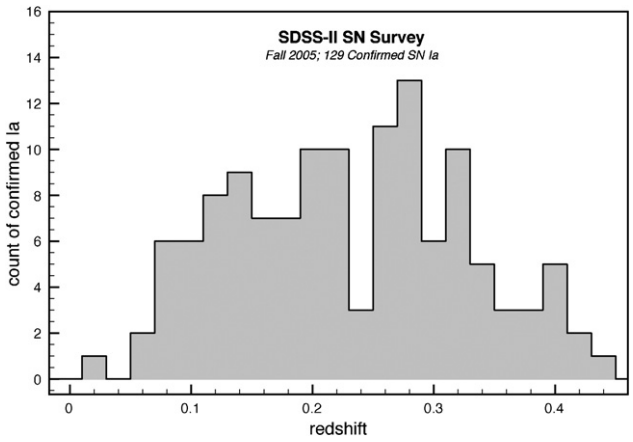

Figure 1. The redshift distribution of 129 spectroscopically confirmed SNe Ia in 2005.

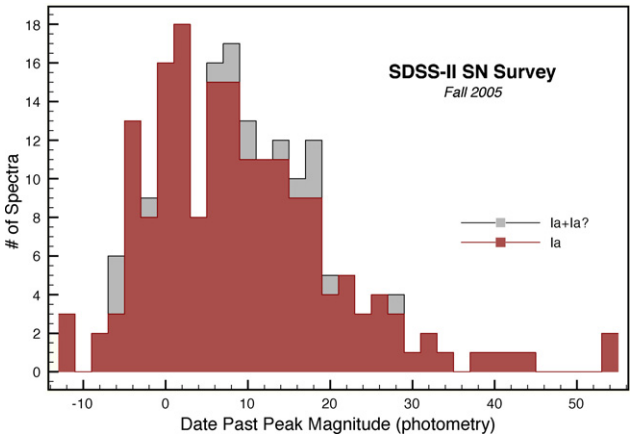

Figure 2. Distribution of first spectroscopy epoch, relative to B-band maximum light, for spectroscopically confirmed and probable SNe Ia; most spectra were obtained before +20 d.

(A color version of this figure is available in the online journal)

SNe Ia, 16 probable SNe Ia, 7 SNe Ib/c, and 11 SNe II. Figure 1 shows the redshift distribution of the confirmed SNe Ia. The distribution is approximately flat for $0.1 < z < 0.35$ with a deficit at $z \approx 0.2$. This deficit is almost purely a result of bias in our follow-up selection, with bright low-z sources assigned to the smaller telescopes and distant sources targeted at the $\geqslant$8 m facilities.

Most SNe had spectroscopy within 20 d of photometric maximum (Figure 2). Multi-epoch follow-up spectroscopy was carried out for the peculiar Type Ia SN 2005js (two epochs; similar to SN 1991bg—e.g., Filippenko et al. 1992b), the underluminous, low-expansion velocity Type Ia SN 2005hk (ten epochs; see also Chornock et al. 2006; Phillips et al. 2007), and a peculiar event, SN 2005gj (23 epochs; see also Aldering et al. 2006; Prieto et al. 2007), which had broad SN Ia-like features with superimposed hydrogen emission lines (similar to SN 2002ic, Hamuy et al. 2003). Three broad-lined Type Ic "hypernovae" (similar to SN 1998bw and SN 2002ap; e.g., Stathakis et al. 2000; Foley et al. 2003) were observed as well: SN 2005fk, SN 2005kr, and SN 2005ks, selected as Type Ic "hypernovae" based on their light curves, each had a SN 2002ap-like spectrum. At least some "hypernovae" are believed to be associated with gamma-ray bursts (e.g., Stanek et al. 2003; Matheson et al. 2003).

Here we summarize the observing configurations for the main facilities. The individual targeted SN positions and dates of observations are listed in Table 1.

3.1. Telescopes

3.1.1. MDM 2.4 m

The MDM 2.4 m telescope was used for both imaging and spectroscopy of the SN candidates. With a large number of nights and an efficient spectrograph, this facility made important contributions despite its modest aperture. Spectra were taken with the Boller & Chivens CCD Spectrograph (CCDS), with a 150 l mm^{-1} grating (4700 Å blaze) feeding a 1200 × 800 Loral CCD. With a 2″ slit we obtained a resolution of 15 Å covering ∼3800–7300 Å. Observations with the fixed north/south slit were taken within 1 h of transit, whenever possible, to minimize refractive slit losses (Filippenko 1982). Typically the exposure was 3 × 900 s. A total of 38 spectra were obtained confirming 16 SNe Ia, two SNe Ib/c, and four host galaxies, with a redshift distribution centered at $z \approx 0.08$. This telescope was used extensively to perform multi-epoch spectroscopy of bright, nearby events.

3.1.2. ARC 3.5 m

The 54 ARC spectra were obtained with the Dual Imaging Spectrograph (DIS), which has dual (red/blue) cameras with Marconi 2048 × 1024 pixel back-illuminated chips. The blue spectra used a 300 l mm^{-1} grating giving 2.43 Å pixel^{-1} centered at 4224 Å; the red camera employed a 300 l mm^{-1} grating for 2.26 Å pixel^{-1} dispersion, centered at 7500 Å. With a slit width of ∼1.5″, the effective resolution was ∼8–9 Å. For most observations with a visible host, the slit was aligned with the SN and galaxy core. Typical exposures were 300–900 s and 3–5 exposures were combined for the final spectra. The observations yielded 38 SNe (29 SNe Ia, three probable SNe Ia, five SNe II, and one SN Ib), with a median redshift of ∼0.11.

3.1.3. HET 9.2 m

The HET was used to observe SN candidates with higher photo-z. Exposures were made with the Marcario Low-Resolution Spectrograph (LRS; Hill et al. 1998), employing a Ford Aerospace 3072 × 1024 pixel chip and the 300 l mm^{-1} G1 grism for a dispersion of 5 Å pixel^{-1}. With a slit width of 2″, the effective resolution was ∼20 Å. Observations were made with the slit at the parallactic angle (Filippenko 1982) to avoid differential slit losses and improve (relative) spectrophotometry across the range 4067–10700 Å. As the HET is queue scheduled (Shetrone et al. 2007), many SN spectra were obtained soon after discovery, and lower-priority observation time was spent acquiring late-time data for SNe with previous spectroscopic confirmation. We obtained 92 HET spectra over a period of 69 days, yielding 61 SNe (45 SNe Ia, 10 probable SNe Ia, one SN Ib, two SNe II, and three SNe Ibc) with a redshift distribution centered at $z \approx 0.27$. A few multi-epoch observations and a few unclassifiable spectra completed the sample.

3.1.4. WHT 4.2 m

Six nights of observing were obtained with the ISIS Double Beam Spectrograph. Spectra with a combined red/blue coverage of 3900–8900 Å were obtained for 30 SN candidates. Typically

Table 1
SDSS-II SN Spectroscopic Follow-up Observations

IAU[a] Name	SNID[b]	R.A. (J2000)	Decl. (J2000)	Telescope	Obs. Date (UT)
2005ed	722	00 02 49.36	+00 45 04.8	APO	2005 Sep 09
2005ef	739	00 58 22.87	+00 40 44.6	APO	2005 Sep 09
2005ei	744	21 56 47.65	+00 19 03.0	APO	2005 Sep 08
2005eg	762	01 02 08.49	−00 52 44.5	APO	2005 Sep 09
2005ex	774	01 41 51.24	−00 52 35.0	APO	2005 Sep 09
2005ex	774	01 41 51.24	−00 52 35.0	MDM	2005 Sep 15
...	779	01 46 41.70	−01 01 14.1	HET	2005 Dec 29
2005ez	1032	03 07 10.97	+01 07 10.4	APO	2005 Sep 25
2005fg	1112	22 36 04.20	−00 22 30.8	HET	2005 Sep 26
2005lb	1114	22 54 50.06	−00 15 08.9	APO	2005 Nov 04
2005fc	1119	21 21 39.25	+00 53 40.7	Subaru	2005 Sep 27
...	1166	00 37 25.35	+00 58 23.8	Subaru	2005 Sep 28
2005ff	1241	22 30 41.41	−00 46 35.7	WHT	2005 Sep 23
2005fd	1253	21 35 11.76	+00 09 47.3	WHT	2005 Sep 24
2005fd	1253	21 35 11.76	+00 09 47.3	APO	2005 Sep 24
2005fd	1253	21 35 11.76	+00 09 47.3	HET	2005 Sep 26
2005fe	1316	22 19 27.32	+00 29 39.9	WHT	2005 Sep 29
2005fh	1371	23 17 29.71	+00 25 45.8	APO	2005 Sep 25
...	1461	01 37 29.44	+00 12 35.0	HET	2005 Dec 31
2005lc	1472	03 02 11.19	−01 09 59.4	APO	2005 Nov 06
...	1525	03 08 49.93	+00 09 30.0	HET	2005 Dec 25
...	1545	00 57 42.28	−00 40 42.3	APO	2005 Sep 09
2005fb	1580	03 01 17.54	−00 38 38.6	WHT	2005 Sep 23
...	1595	21 26 16.29	−00 33 14.6	MDM	2005 Sep 25
...	1632	21 30 54.23	−00 08 02.2	APO	2005 Sep 28
...	1686	00 08 59.60	−00 12 37.5	Subaru	2005 Sep 27
...	1688	21 25 25.85	+00 19 28.3	Subaru	2005 Sep 28
...	1740	00 21 37.06	−00 52 51.1	HET	2005 Dec 25
2005fj	1794	21 11 20.85	−00 26 43.3	WHT	2005 Sep 24
2005hl	2000	20 55 19.79	+00 32 34.7	MDM	2005 Oct 22
2005fo	2017	21 55 46.40	+00 35 36.7	HET	2005 Sep 22
2005fl	2030	20 47 21.99	−01 15 11.9	HET	2005 Sep 27
2005fm	2031	20 48 10.37	−01 10 17.1	WHT	2005 Sep 23
2005fk	2053	21 15 19.84	−00 22 58.6	HET	2005 Sep 27
...	2063	21 59 23.79	−01 06 27.0	HET	2005 Sep 25
2005fn	2102	20 48 53.05	+00 11 28.0	APO	2005 Sep 27
2005fr	2165	01 08 22.02	−00 05 46.7	Subaru	2005 Sep 29
2005fy	2246	03 20 21.70	−00 53 08.1	APO	2005 Sep 25
2005fy	2246	03 20 21.70	−00 53 08.1	WHT	2005 Sep 25
2005ey	2308	02 17 05.50	+00 16 48.9	WHT	2005 Sep 23
2005fp	2330	00 27 13.69	+01 07 14.2	Subaru	2005 Sep 28
2005fq	2366	00 53 44.05	−00 33 36.8	HET	2005 Oct 01
...	2371	02 39 58.49	−00 31 49.4	APO	2005 Nov 06
2005ft	2372	02 42 04.98	−00 32 27.0	WHT	2005 Sep 24
2005ft	2372	02 42 04.98	−00 32 27.0	APO	2005 Sep 25
2005fi	2422	00 07 58.69	+00 38 17.4	Subaru	2005 Sep 28
2005fu	2440	02 50 32.09	+00 48 28.1	WHT	2005 Sep 24
2005fs	2533	02 04 52.98	−00 19 35.2	HET	2005 Oct 01
2005fv	2561	03 05 22.42	+00 51 30.1	MDM	2005 Sep 24
2005fv	2561	03 05 22.42	+00 51 30.1	WHT	2005 Sep 24
2005fv	2561	03 05 22.42	+00 51 30.1	APO	2005 Sep 25
2005fv	2561	03 05 22.42	+00 51 30.1	MDM	2005 Sep 25
2005fw	2635	03 30 49.04	−01 14 17.2	WHT	2005 Sep 25
2005fw	2635	03 30 49.04	−01 14 17.2	Subaru	2005 Oct 27
...	2661	23 32 49.81	+00 05 49.9	Subaru	2005 Sep 28
2005fa	2689	01 39 36.09	−00 45 31.5	WHT	2005 Sep 23
2005hm	2744	21 39 00.65	−01 01 38.7	MDM	2005 Oct 24
...	2746	02 18 25.13	+01 08 00.9	APO	2005 Sep 25
...	2746	02 18 25.13	+01 08 00.9	WHT	2005 Sep 26
2005fx	2789	22 56 48.34	+00 24 03.9	Subaru	2005 Sep 27
...	2864	23 57 48.24	−01 14 22.6	HET	2005 Dec 22
2005fz	2916	21 03 41.22	+00 34 10.3	WHT	2005 Sep 26
2005fz	2916	21 03 41.22	+00 34 10.3	APO	2005 Sep 27
2005fz	2916	21 03 41.22	+00 34 10.3	APO	2005 Oct 01

Table 1
(Continued)

IAU[a] Name	SNID[b]	R.A. (J2000)	Decl. (J2000)	Telescope	Obs. Date (UT)
...	2928	00 19 24.60	−00 35 20.8	HET	2005 Dec 29
...	2929	00 36 02.88	−00 50 06.0	MDM	2005 Sep 25
2005go	2943	01 10 49.18	+01 00 28.4	HET	2005 Oct 09
2005gp	2992	03 41 59.29	−00 46 57.6	APO	2005 Oct 07
2005gp	2992	03 41 59.29	−00 46 57.6	Subaru	2005 Oct 26
2005ga	3080	01 07 43.76	−01 02 22.2	WHT	2005 Sep 26
2005ga	3080	01 07 43.76	−01 02 22.2	APO	2005 Sep 28
2005ga	3080	01 07 43.76	−01 02 22.2	Subaru	2005 Oct 27
2005gc	3087	01 21 37.62	−00 58 38.0	MDM	2005 Oct 03
2005gs	3199	22 13 10.25	+01 03 02.1	HET	2005 Oct 09
2005gh	3241	20 50 36.35	−00 21 14.8	WHT	2005 Sep 30
2005hn	3256	21 57 04.23	−00 13 24.4	MDM	2005 Oct 25
2005gd	3317	01 47 51.03	+00 38 26.2	APO	2005 Sep 27
2005ge	3331	02 18 14.73	+00 47 47.6	WHT	2005 Sep 26
2005gr	3377	03 36 37.49	+01 04 45.0	HET	2005 Oct 12
2005gf	3451	22 16 16.61	+00 42 29.5	Subaru	2005 Sep 27
2005gg	3452	22 18 41.16	+00 38 21.1	Subaru	2005 Sep 27
...	3508	01 03 17.71	−00 10 44.4	HET	2005 Dec 20
...	3508	01 03 17.71	−00 10 44.4	HET	2005 Dec 25
...	3535	02 56 28.13	−00 08 00.5	HET	2005 Dec 21
2005gb	3592	01 16 12.58	+00 47 31.0	APO	2005 Sep 27
2005gb	3592	01 16 12.58	+00 47 31.0	MDM	2005 Oct 01
2005gb	3592	01 16 12.58	+00 47 31.0	MDM	2005 Oct 13
2005gi	3818	00 55 52.68	+00 30 17.8	APO	2005 Sep 27
2005ho	3901	00 59 24.10	+00 00 09.3	APO	2005 Sep 28
2005ho	3901	00 59 24.10	+00 00 09.3	MDM	2005 Oct 20
...	3959	03 00 23.50	+00 30 42.8	HET	2005 Dec 30
...	4000	02 04 03.84	−00 21 56.9	HET	2005 Oct 10
2005gt	4012	03 13 47.74	−00 14 37.0	WHT	2005 Oct 24
2005gw	4046	23 37 59.60	+00 38 31.7	HET	2005 Oct 10
...	4064	03 04 26.32	+01 02 47.1	APO	2005 Oct 07
...	4236	00 07 37.36	−01 01 06.0	HET	2005 Dec 23
2005gu	4241	00 48 57.05	−00 54 20.8	HET	2005 Oct 10
...	4281	02 13 28.18	−00 58 05.7	APO	2005 Oct 05
...	4307	01 59 51.00	−00 56 58.9	HET	2005 Dec 21
...	4311	02 08 31.43	+01 01 11.9	HET	2005 Dec 22
2005gj	4524	03 01 11.96	−00 33 13.9	MDM	2005 Oct 01
2005gj	4524	03 01 11.96	−00 33 13.9	APO	2005 Oct 03
2005gj	4524	03 01 11.96	−00 33 13.9	APO	2005 Oct 07
2005gj	4524	03 01 11.96	−00 33 13.9	MDM	2005 Oct 12
2005gj	4524	03 01 11.96	−00 33 13.9	MDM	2005 Oct 22
2005gj	4524	03 01 11.96	−00 33 13.9	MDM	2005 Oct 25
2005gj	4524	03 01 11.96	−00 33 13.9	MDM	2005 Nov 02
2005gj	4524	03 01 11.96	−00 33 13.9	WHT	2005 Nov 10
2005gj	4524	03 01 11.96	−00 33 13.9	MDM	2005 Nov 12
2005gj	4524	03 01 11.96	−00 33 13.9	WHT	2005 Nov 12
2005gj	4524	03 01 11.96	−00 33 13.9	MDM	2005 Nov 26
2005gj	4524	03 01 11.96	−00 33 13.9	MDM	2005 Nov 28
2005gj	4524	03 01 11.96	−00 33 13.9	MDM	2005 Dec 08
2005gj	4524	03 01 11.96	−00 33 13.9	MDM	2005 Dec 25
2005gv	4577	02 33 54.13	+00 16 50.6	HET	2005 Oct 08
...	4676	01 15 17.68	+00 47 17.5	HET	2005 Dec 21
2005gy	4679	01 26 06.79	+00 40 36.8	HET	2005 Oct 08
2005gx	5103	23 59 32.27	+00 44 13.7	APO	2005 Oct 05
2005gq	5183	03 33 48.97	+00 42 33.7	HET	2005 Oct 08
2005hp	5350	20 28 52.60	−00 46 45.4	HET	2005 Oct 22
...	5378	02 30 56.86	−01 15 07.5	MDM	2005 Dec 26
2005hs	5391	03 29 22.06	−01 05 41.0	Subaru	2005 Oct 26
2005hr	5395	03 18 33.81	+00 07 24.3	MDM	2005 Oct 23
2005hu	5533	21 54 40.80	+00 24 47.8	Subaru	2005 Oct 26
2005hx	5549	00 13 00.13	+00 14 53.7	MDM	2005 Oct 22
2005hy	5550	00 14 23.59	+00 19 59.1	WHT	2005 Oct 24
2005hw	5588	00 09 28.47	+01 09 17.6	HET	2005 Oct 27
2005hv	5635	22 12 43.86	−00 02 05.6	WHT	2005 Oct 24

Table 1
(Continued)

IAU[a] Name	SNID[b]	R.A. (J2000)	Decl. (J2000)	Telescope	Obs. Date (UT)
...	5673	23 35 12.32	+00 47 03.6	HET	2005 Oct 26
2005ia	5717	01 11 35.02	−00 00 21.0	Subaru	2005 Oct 27
2005jz	5736	01 31 27.07	−00 37 54.0	HET	2005 Nov 05
2005ib	5737	01 31 25.70	−00 36 12.3	Subaru	2005 Oct 27
2005hz	5751	00 46 32.18	+00 50 18.1	WHT	2005 Oct 24
2005hz	5751	00 46 32.18	+00 50 18.1	Subaru	2005 Nov 27
2005hq	5821	20 50 19.78	−00 49 31.0	HET	2005 Oct 25
2005hq	5821	20 50 19.78	−00 49 31.0	HET	2005 Oct 27
2005ic	5844	21 51 08.69	−00 50 34.6	Subaru	2005 Oct 26
2005is	5916	00 21 44.97	−00 19 30.0	MDM	2005 Oct 25
2005is	5916	00 21 44.97	−00 19 30.0	APO	2005 Oct 31
2005hc	5944	01 56 47.94	−00 12 49.1	MDM	2005 Oct 22
2005hc	5944	01 56 47.94	−00 12 49.1	MDM	2005 Oct 24
2005hc	5944	01 56 47.94	−00 12 49.1	Subaru	2005 Nov 27
2005ie	5957	02 19 02.53	−00 16 22.0	Subaru	2005 Oct 26
...	5963	00 44 19.45	+00 28 46.2	HET	2005 Dec 23
2005it	5966	01 04 45.69	+00 30 50.1	HET	2005 Oct 30
...	5993	01 58 43.77	+00 02 56.7	HET	2005 Dec 25
2005ht	5994	20 50 24.60	−00 10 04.4	WHT	2005 Oct 24
2005if	6057	03 30 12.87	−00 58 28.5	MDM	2005 Oct 23
2005if	6057	03 30 12.87	−00 58 28.5	Subaru	2005 Nov 26
2005ka	6100	22 13 55.96	+01 05 11.4	HET	2005 Nov 04
2005ih	6108	00 07 13.58	+00 20 56.3	Subaru	2005 Oct 28
2005iw	6127	22 29 17.75	−00 05 32.4	HET	2005 Oct 30
2005iv	6137	20 31 44.68	+00 14 41.1	HET	2005 Nov 02
2005jy	6192	23 13 51.60	+01 15 25.2	HET	2005 Nov 05
2005ig	6196	22 30 31.47	−00 30 09.5	Subaru	2005 Oct 27
2005ii	6249	00 13 03.73	−00 37 12.4	Subaru	2005 Oct 28
2005js	6295	01 34 41.51	−00 36 19.4	HET	2005 Nov 07
2005jk	6304	01 45 59.43	+01 11 45.4	APO	2005 Nov 05
2005jk	6304	01 45 59.43	+01 11 45.4	Keck	2005 Nov 05
2005ix	6315	20 41 55.88	+01 05 31.3	HET	2005 Nov 01
2005ix	6315	20 41 55.88	+01 05 31.3	Keck	2005 Nov 05
2005ij	6406	03 04 21.26	−01 03 46.6	WHT	2005 Oct 24
2005ij	6406	03 04 21.26	−01 03 46.6	Subaru	2005 Nov 26
2005id	6422	23 16 33.32	−00 39 47.6	WHT	2005 Oct 24
...	6471	20 37 32.67	+00 29 41.8	Subaru	2005 Oct 28
2005hj[c]	6558	01 26 48.40	−01 14 17.2	HET	2005 Oct 26
2005jd	6649	02 17 06.21	+00 32 05.3	HET	2005 Nov 01
2005jd	6649	02 17 06.21	+00 32 05.3	Keck	2005 Nov 05
...	6696	22 36 19.04	+00 28 45.3	HET	2005 Oct 31
2005ik	6699	21 31 15.60	−01 03 25.2	Subaru	2005 Oct 28
2005ik	6699	21 31 15.60	−01 03 25.2	Keck	2005 Nov 05
...	6714	23 49 26.41	+00 37 54.8	HET	2005 Dec 20
2005iu	6773	20 20 15.60	+00 13 02.6	APO	2005 Oct 31
2005iy	6777	21 24 51.94	+00 23 08.2	HET	2005 Oct 30
2005iy	6777	21 24 51.94	+00 23 08.2	HET	2005 Nov 02
2005iz	6780	21 52 16.47	+00 16 01.5	HET	2005 Nov 01
2005jf	6852	03 33 40.76	−00 06 43.6	HET	2005 Oct 31
2005ja	6924	23 55 52.64	+00 52 37.1	HET	2005 Oct 31
2005jc	6933	00 45 24.41	+01 04 32.1	APO	2005 Nov 02
2005jc	6933	00 45 24.41	+01 04 32.1	Keck	2005 Nov 05
2005jl	6936	21 32 56.12	−00 41 59.2	Keck	2005 Nov 05
2005je	6962	02 35 26.61	+01 04 29.6	APO	2005 Nov 02
...	6968	01 18 13.37	−00 54 23.6	APO	2005 Nov 24
...	7017	02 05 27.68	−00 29 52.5	APO	2005 Nov 02
...	7099	22 51 33.17	+01 10 02.5	APO	2005 Oct 31
...	7102	21 38 28.78	−00 36 56.1	APO	2005 Oct 31
2005jg	7143	23 01 02.97	−00 12 26.7	HET	2005 Nov 01
2005jh	7147	23 20 04.42	−00 03 19.8	MDM	2005 Nov 03
2005jh	7147	23 20 04.42	−00 03 19.8	Keck	2005 Nov 05
2005jm	7243	21 52 18.97	+00 28 19.1	Keck	2005 Nov 05
2005kn	7335	21 15 32.45	−00 21 19.2	HET	2005 Nov 09
2005jb	7426	22 36 03.21	−00 22 04.5	HET	2005 Oct 31

Table 1
(Continued)

IAU[a] Name	SNID[b]	R.A. (J2000)	Decl. (J2000)	Telescope	Obs. Date (UT)
...	7444	01 50 48.71	−00 25 47.4	HET	2005 Dec 19
2005jx	7460	21 34 20.18	−00 40 54.0	HET	2005 Nov 04
2005ji	7473	00 17 18.34	−00 15 26.1	MDM	2005 Nov 04
2005ji	7473	00 17 18.34	−00 15 26.1	Keck	2005 Nov 05
2005jn	7475	00 19 00.84	−00 16 53.3	HET	2005 Nov 05
2005jn	7475	00 19 00.84	−00 16 53.3	Keck	2005 Nov 05
2005jo	7512	03 28 21.68	−00 19 34.1	Keck	2005 Nov 05
...	7647	23 53 31.95	+01 02 31.3	HET	2005 Dec 21
2005jw	7779	20 40 19.25	−00 00 25.9	HET	2005 Nov 05
2005jp	7847	02 09 50.38	−00 03 42.2	Keck	2005 Nov 05
2005ir	7876	01 16 43.80	+00 47 40.7	APO	2005 Nov 02
2005ir	7876	01 16 43.80	+00 47 40.7	APO	2005 Nov 06
...	7922	02 12 53.30	−00 55 03.1	HET	2005 Nov 02
2005jj	7947	20 56 44.66	+00 24 30.0	HET	2005 Nov 03
2005jv	8030	02 40 50.12	+00 59 35.2	HET	2005 Nov 05
2005ju	8046	02 36 28.04	+00 30 40.6	HET	2005 Nov 04
2005hk	8151	00 27 50.89	−01 11 53.3	MDM	2005 Nov 03
2005hk	8151	00 27 50.89	−01 11 53.3	APO	2005 Nov 04
2005hk	8151	00 27 50.89	−01 11 53.3	MDM	2005 Nov 04
2005hk	8151	00 27 50.89	−01 11 53.3	APO	2005 Nov 06
2005hk	8151	00 27 50.89	−01 11 53.3	WHT	2005 Nov 10
2005hk	8151	00 27 50.89	−01 11 53.3	WHT	2005 Nov 12
2005hk	8151	00 27 50.89	−01 11 53.3	MDM	2005 Nov 14
2005hk	8151	00 27 50.89	−01 11 53.3	MDM	2005 Dec 07
2005ko	8213	23 50 05.03	−00 55 17.1	HET	2005 Nov 21
2005mi	8495	22 21 02.65	−00 44 53.4	HET	2005 Dec 07
2005jt	8598	02 50 40.17	−00 03 57.5	HET	2005 Nov 06
2005jr	8679	01 00 12.37	+00 20 26.9	Keck	2005 Nov 05
2005mh	8707	02 44 56.67	+00 12 13.2	HET	2005 Dec 07
2005kp	8719	00 30 53.15	−00 43 07.9	APO	2005 Nov 09
...	8742	00 44 57.49	+00 26 14.2	HET	2005 Dec 31
2005ld	8921	21 40 00.47	−00 00 28.5	APO	2005 Nov 24
2005le	9032	22 31 32.29	−00 29 36.8	Subaru	2005 Nov 26
2005kq	9045	23 11 20.91	−00 36 31.0	HET	2005 Nov 22
2005kr	9118	03 08 29.67	+00 53 20.2	HET	2005 Nov 22
2005lg	9207	01 16 20.07	−00 48 28.1	Subaru	2005 Nov 26
2005ks	9273	21 37 56.56	−00 01 56.9	HET	2005 Nov 22
2005li	9457	22 23 15.45	+00 15 11.0	HET	2005 Nov 23
2005lh	9467	21 55 48.33	+01 10 51.0	HET	2005 Dec 01
...	9954	00 26 20.19	−00 25 31.6	HET	2005 Dec 26
2005kt	10028	01 10 58.04	+00 16 34.2	WHT	2005 Nov 12
...	10045	21 48 46.84	+01 12 41.2	HET	2005 Nov 27
2005lj	10096	01 57 43.04	−00 10 46.0	APO	2005 Nov 26
...	10106	03 10 46.39	−00 12 17.6	HET	2005 Dec 28
2005mk	10297	22 42 40.63	+00 49 58.9	HET	2005 Dec 04
2005kb	10367	00 50 50.68	+00 51 13.0	APO	2005 Nov 09
2005lk	10434	21 59 49.42	−01 11 37.4	APO	2005 Nov 24
2005ll	10449	22 28 06.88	−01 07 41.6	Subaru	2005 Nov 27
2005lf	10550	23 18 42.09	−01 12 17.6	Subaru	2005 Nov 26
2005ku	10805	22 59 42.61	−00 00 49.4	MDM	2005 Nov 22
2005lm	10907	00 15 04.91	+00 21 18.6	APO	2005 Nov 24
...	10915	01 21 52.25	+00 23 19.9	HET	2005 Dec 23
...	10928	00 26 42.53	−00 48 13.8	APO	2005 Nov 26
...	10976	01 28 40.94	−00 53 21.2	APO	2005 Nov 26
2005mj[d]	11017	21 31 49.44	−01 04 09.9	Magellan	2005 Nov 19
2005ml	11067	02 14 04.41	−00 14 21.0	APO	2005 Dec 04
2005mm	11206	00 13 09.55	+01 08 43.9	HET	2005 Dec 03
2005ln	11300	00 27 00.12	−00 35 11.8	APO	2005 Nov 24
2005mo	11320	03 50 12.90	−00 14 24.9	HET	2005 Dec 07
2005mn	11332	03 49 18.44	−00 41 31.5	HET	2005 Dec 01
2005mn	11332	03 49 18.44	−00 41 31.5	APO	2005 Dec 04
2005mn	11332	03 49 18.44	−00 41 31.5	HET	2005 Dec 07
2005mn	11332	03 49 18.44	−00 41 31.5	HET	2005 Dec 30
2005lo	11452	00 37 11.87	−01 12 12.4	HET	2005 Dec 02
2005lq	11557	02 41 36.05	+00 12 18.0	HET	2005 Dec 01
2005mp	11650	01 04 45.67	+00 03 20.3	HET	2005 Dec 03
2005lp	11864	01 47 42.80	+00 12 25.9	HET	2005 Dec 01
2005mq	12136	23 20 21.78	−00 20 59.6	HET	2005 Dec 07

Notes.
[a] Official IAU name, when assigned.
[b] SDSS Internal SN candidate ID.
[c] Spectroscopically confirmed by another group using the HET (CBET 266; Quimby et al. 2007). The spectrum is not available.
[d] Spectroscopically confirmed by the ESSENCE group.

the slit width was set at 1″, providing a resolution of 4.3 Å in the blue and 7.5 Å in the red, although the slit was adjusted to accommodate variable seeing. For the observations in October and November, a GG495 filter was employed in the red channel to eliminate second-order contamination. The observations provided 26 SNe Ia, three probable SNe Ia, and one SN Ic (with a median SN redshift of ∼0.16).

3.1.5. Subaru 8.2 m

At this telescope we used the Faint Object Camera and Spectrograph (FOCAS), taking advantage of the excellent image quality to employ a 0.8″ slit and target higher-redshift SNe with significant host-galaxy contamination. Separate exposures were made using blue and red 300 l mm^{-1} grisms. The blue setting covered 3650–6000 Å, while the red covered 4900–9000 Å. The resulting resolution was ∼8–12 Å. Typical exposures of 3 × 300 s allowed us to confirm 30 SNe Ia, one probable SN Ia, and two SNe II, with a median redshift of ∼0.25.

3.1.6. Keck 10 m

One target-of-opportunity night (2005 November 5) was obtained with the Low-Resolution Imaging Spectrograph (LRIS; Oke et al. 1995) on Keck I. The blue side covered ∼3200–5700 Å with a 600 l mm^{-1} grating (4000 Å blaze; 1.92 Å pixel^{-1} dispersion), and the red side covered ∼5500–9400 Å with a 400 l mm^{-1} grating (8500 Å blaze; 0.61 Å pixel^{-1} dispersion). A slit of width 1″ was oriented at the parallactic angle for an effective resolution of 8.9 Å (blue) and 4.5 Å (red). With exposures ranging from 700 to 2400 s, we observed 12 SNe Ia and one SN IIn; the median redshift was ∼0.24. Most of these objects had been previously confirmed as spectroscopic SNe Ia at our other telescopes, but the Keck spectra generally had higher signal-to-noise ratio (S/N) and provided important rest-frame UV information on the SNe.

3.2. Calibrations and Reductions

Basic data calibration (bias/overscan subtraction, flux calibration, and wavelength calibration) was performed by the individual observing teams using standard IRAF[49] routines. SN spectra were extracted from the geometrically corrected two-dimensional (2D) spectra, often with significant amounts of

[49] IRAF is distributed by the National Optical Astronomy Observatory, which is operated by the Association of Universities for Research in Astronomy, Inc., under cooperative agreement with the National Science Foundation.

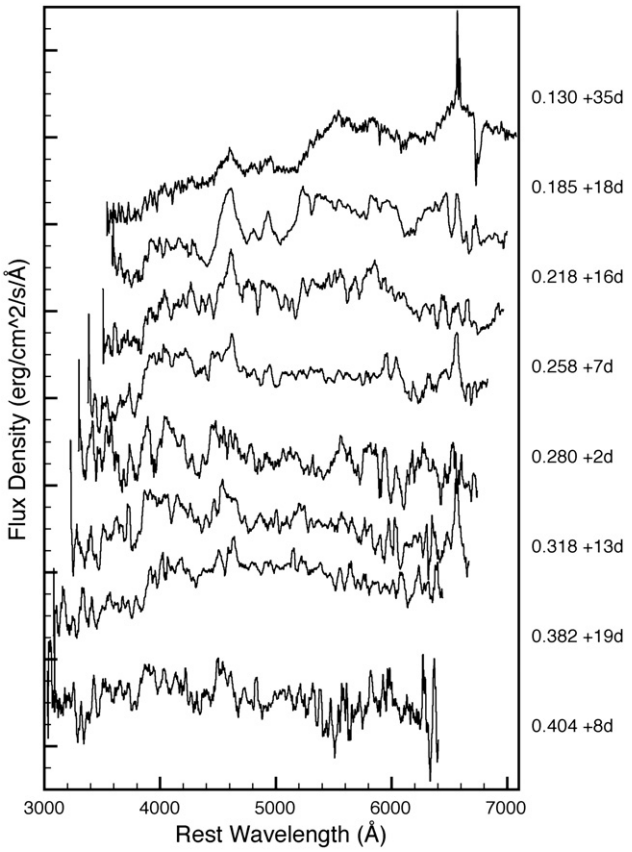

Figure 3. A sample of observed Ia spectra from the fall 2005 run with significant host-galaxy contamination. All spectra have been shifted to the rest frame (numbers at right give the redshifts and epochs relative to B-band maximum) and have been normalized for display purposes. The top spectrum (from Subaru) has not been corrected for telluric absorption.

host-galaxy background (see Figure 3); for higher-z targets embedded in their hosts, modest spatial-width apertures were used in extracting the SN spectra to minimize host contamination. In half of the cases, a separate host-dominated aperture could be extracted from the 2D spectrum to produce a host-galaxy spectrum. For ARC observations, a separate host-core aperture was often extracted. For the other observations, the near parallactic orientation minimized chromatic slit losses; however, given our narrow slits and extraction apertures, no attempt at absolute spectrophotometry was made. Reductions of the HET, ARC, WHT, and Keck data included a correction for telluric absorption.

4. SN IDENTIFICATION

The principal goal of the spectroscopic observations is to classify the SN and measure its redshift. We can also use these measurements to improve the choice of future spectroscopic targets. For low-z SNe with high-S/N spectra, the classification is, in principle, simple (Filippenko 1997)—Type II show strong Balmer lines, Type Ia show strong Si II lines, Type Ib lack H lines but show strong He emission, Type Ic lack all of the above. Traditional classification is done by visual inspection. In practice, however, our spectra have a widely varying S/N, cover a large redshift range, and suffer significant host-galaxy contamination and extinction. Further, with this large, relatively unbiased sample, we expect rare, "peculiar" SNe to be present (which are not discussed further in the present paper, but will be part of a future analysis with the complete spectroscopic sample). We have sought to develop automatic classification programs capable of dealing with our sample, exploring template cross-correlation and principal component analysis (PCA) techniques. While these have substantial discriminating power and also serve to find best-fitted parameters and their associated statistical errors, the final object (SN- and host-type) classification required some human judgment in at least half of the cases.

Of course, we also need to obtain the accurate redshifts required when using the SNe for cosmology and population studies. These were robustly measured in the cross-correlation analysis, especially in the ∼50% of the spectra with large host-galaxy contamination or separate host spectra. These are augmented by "host-only" spectra, obtained for SNe that had faded before spectroscopy could be arranged (these sources are not discussed further in the present paper). When cross correlation could be locked to the narrow-line host features, we refer to the result as a "galaxy redshift;" these have a typical error of $\delta z \approx 0.0005$. In other cases, we could only match the broad blueshifted SN features; the resulting redshifts ($z_{\rm SN}$) vary in quality, with $\delta z \sim 0.005$ (see discussion below).

In the following sections, we discuss these classification efforts along with our work to model and remove the host-galaxy contamination and extinction. The result is a set of "clean" SN spectra with estimates of the quality of the host subtraction and measurements of the agreement with standard templates of the best-fitting SN type. The latter may be used to flag SNe with significant spectral anomalies, useful in improving our understanding of SN physics and improving our calibration of the SN luminosities.

4.1. Cross-Correlation Analysis

With a suitable set of templates, cross-correlation analysis provides a well-established way to measure redshift and to constrain the spectral type. In the method developed by Tonry & Davis (1979), one computes the cross correlation $c(n) = s(n) * t(n)$ of the original s and template t spectra at zero redshift, after scaling the wavelength axis of $t(n)$ by a factor of $(1+z)$. First the spectra are continuum subtracted, $\ln(\lambda)$ binned, endmasked, and filtered to remove any intrinsic color dependence, low-frequency spectral variations, and high-frequency noise beyond the resolution. The data are trimmed to a range appropriate to each telescope/spectrograph combination to avoid the low-S/N ends and regions where sky-subtraction errors dominate (e.g., we truncate HET spectra at 8300 Å). The code determines the wavelength shift from a fit to the correlation peak; a measure of the fit quality comes from r, the ratio of peak height h to the root-mean square (rms), and σ_a, of the antisymmetric component of $c(n)$ about the correlation redshift. For sufficiently large r (typically > 3; Tonry & Davis 1979; Blondin et al. 2007; Blondin & Tonry 2007), and sufficiently large overlap of s and t in wavelength (defined as the portion of spectrum used for cross correlation; Blondin et al. 2007; Blondin & Tonry 2007), the measurement of the shift is deemed significant.

In our analysis we use the "rvsao.xcsao" cross-correlation package of IRAF. Our SN templates are from Peter Nugent's spectral library[50] (see Nugent et al. 2002, and the SUSPECT database;[51] Table 2). Specifically for the SNe Ia, we used

[50] http://supernova.lbl.gov/∼nugent/nugent_templates.html.
[51] http://bruford.nhn.ou.edu/∼suspect/index1.html.

Table 2
Cross-Correlation Templates From SUSPECT SN Database

Type	Object
Ibc	1954A, 1962L, 1964L, 1990B, 1990I, 1994I, 1998bw, 1999ex, 2000H, 2002ap
II	1948B, 1959D, 1961F, 1961I, 1961V, 1964F, 1964H, 1969L, 1970A, 1986E
II	1987A, 1988A, 1988H, 1988Z, 1989C, 1990ae, 1990ag, 1990E, 1990H, 1990K
II	1990Q, 1990V, 1990X, 1991C, 1991H, 1991J, 1992aa, 1992ab, 1992C, 1992H
II	1993J, 1994aj, 1996L, 1997ab, 1997cy, 1997D, 1998dn, 1998S, 1999em, 2004dj
Ia-pec	1957A, 1960H, 1986G, 1991bg, 1991bj, 1991F, 1991T, 1997br, 1997cn, 1999aa
Ia-pec	1999ac, 1999by, 2000cx

Nugent's Branch-normal (Branch et al. 1993), SN 1991T-like (e.g., Filippenko et al. 1992a), and SN 1991bg-like (e.g., Filippenko et al. 1992b) templates (supplemented by spectra of some peculiar SNe Ia (e.g., SN 1999aa, Garavini et al. 2004; SN 1999by, Garnavich et al. 2004, etc) from SUSPECT. For SNe Ib/c, the templates used are Nugent's normal SN Ib/c and hypernova spectra, as well as observed spectra of SN 1990B (Matheson et al. 2001), SN 1990I (Elmhamdi et al. 2004), SN 1994I (Clocchiatti et al. 1996), SN 1998bw (Ferdinando et al. 2001), SN 1999ex (Hamuy et al. 2002), SN 2000H (Branch et al. 2002), and SN 2002ap (Gal-Yam et al. 2002), from the SUSPECT database). Similarly, the set of Nugent's SN II-P, SN II-L, and SN IIn spectra, augmented by SUSPECT's SN II and peculiar SN II spectra, constitutes the template library for SNe II. These templates represent a variety of SN ages. In particular, the SN Ia templates cover a wide range of epochs (-19 to 70 d from peak B-band magnitude). Galaxy templates were drawn from the SDSS catalog[52] and covered five major morphological types: E/S0, Sa, Sb, Sbc/Sc, and Sm/Im.

When fitting for galaxy redshifts $z_{\rm gal}$, we adjust the xcsao Fourier filtering to focus on narrow features (high frequency in Fourier space). The Fourier cutoff is at a lower frequency when matching SN templates to derive $z_{\rm SN}$. The cross-correlation program provides a best-fitted redshift, r value, and overlap wavelength range for each template in our library. The relative value of r at the best-fitted redshift provides a guide to the best template class. We discard results with less than 40% of the spectra in the overlap region (Blondin et al. 2007; Blondin & Tonry 2007). All measurements are made in the heliocentric frame.

We apply the cross-correlation analysis above to every spectrum obtained and inspect the templates with highest r values and adequate spectral overlap. As expected, the redshift solutions are very insensitive to the template; for example, fits with different galaxy types, such as Sb and Sm/Im, give $\delta z \lesssim 0.001$. SN fits are of course somewhat less precise. Nevertheless, comparing a set of SN Ia and SN Ibc fits gives $\delta z \lesssim 0.005$. Thus, the z measurements reported here are robust. One point deserves comment: half of our spectra have both SN and host-galaxy redshift solutions, and there is a slight, but statistically significant, systematic offset between the two redshifts (see Figure 4). The difference amounts to $\delta z \sim 0.003$ or a velocity shift of $\sim$900 km s^{-1}, which is only a small fraction of the photospheric expansion velocity of the SN ($v \sim 10{,}000$ km s^{-1} near maximum light). Different SNe have different expansion velocities (see, e.g., Benetti et al. 2005) and temporal evolution. Since there is no obvious systematic mismatch between the spectroscopic and photometric epochs (Figure 8), we believe the difference is most likely due to the fact that the average photospheric expansion velocity observed in our SN sample is slightly different from that assumed in Nugent's branch-normal SN Ia templates, which is strictly valid for SN Ia with a stretch factor of unity. When only an SN redshift is available, we correct the $z_{\rm SN}$ for this systematic offset 0.003 (the mean of Figure 4). However, when a significant r is obtained for a galaxy fit $z_{\rm gal}$, we adopt these more accurate redshifts. The dispersion in the $z_{\rm SN}/z_{\rm gal}$ comparison of 0.005 is also adopted here for the systematic error in the $z_{\rm SN}$ measurement. This error is generally larger than the statistical error ($\delta z \approx 0.001$) associated with rvsao.xcsao fit results, as it includes systematics associated with uncertainty in the SN velocity and epoch. We compared our galaxy measurements with redshifts from the SDSS database, where available (about a fifth of our sources, primarily at low redshift), finding agreement to within $\delta z = 0.001$; no systematic offset is observed.

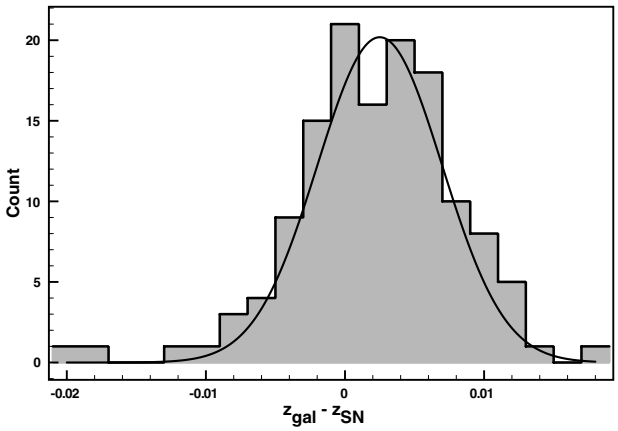

Figure 4. Histogram of $z_g - z_{\rm SN}$ for 136 spectra of 116 SNe in our 2005 data with both host-galaxy and SN redshift solutions. The red line shows a best-fitted Gaussian, with offset $\delta z = 0.003$ and a width of $\sigma_z = 0.005$. The latter is used as an estimate of the error in the SN redshift when narrow host-galaxy lines are not detected.

Comparison of r values between different templates can be used to select the most likely spectral class. For high-quality spectra with little or no host-galaxy contamination, the r values usually cleanly select one SN type. However, for other spectra, we had to visually inspect the solutions at the local r maximum for each SN/galaxy type. This was done by plotting the data over the combined redshifted SN/galaxy spectrum, with a visual normalization, and inspecting how well the features match. Generally, the largest r value was indeed preferred, but in a few cases inspection showed that the largest r corresponded to a misleading fluctuation in the template matches. High-redshift and low-quality spectra, in particular, often showed multiple local minima and human judgment was needed to select the best match. For a small fraction (less than 10%) of our spectra

[52] http://www.sdss.org/dr5/algorithms/spectemplates/index.html.

that have very low S/N ratio, none of these local minima makes a reasonable fit and thus the spectra were classified as "unknown" and not included in this paper.

We found that r did not select as well between host-galaxy classes as between SN types. A clear differentiation between absorption-line-dominated Sa and emission-line-dominated (Irr) spectra is available whenever the S/N and host contamination are fairly large. However, finer distinctions (e.g., Sa/Sb) were not reliable. Indeed, for our multi-epoch spectra, ∼40% of the time the best-fitted host template differs by a class between epochs.

We spectroscopically identified SNe Ia according to the following criteria: (1) $r \geqslant 3$ and (2) a high-significance detection of at least one Si II absorption-line feature (at rest wavelengths of ∼4000 Å, ∼5800 Å, and ∼6150 Å). For lower values ($r \approx 3$), we additionally required a spectrum/template spectral overlap >60% (lower overlap values usually indicate a poor type and redshift range) and/or a host with a spectroscopic classification of E/S0. A requirement of $r \geqslant 3$ for SN Ia identification has also been adopted by other groups (Blondin et al. 2007; Blondin & Tonry 2007; Matheson et al. 2005). When these criteria are satisfied, we designate the SN as Type Ia ("Ia"). When one or more of these criteria fail, but the best match is still a Ia template, we mark the object as "Ia?"—a spectroscopically probable SN Ia. In particular, for late-time spectra the r discrimination was often poor between Types Ia and Ib/c. Occasionally, both SN Ia and SN Ia-pec types gave acceptable fits. In these cases, host-galaxy type, absolute magnitude, and the extent of the spectral overlap were helpful in making the final classification. Thus, while the redshift estimates are quantitative and, for a given spectrum type, choice of the best-fitted SN age is quantitative, the selection of the best-type match is necessarily somewhat subjective.

Once a type is confirmed, we find that the r values resolve the SN phase to an accuracy of ∼2 to 3 d, similar to other SN template-fitting techniques (Balland et al. 2006; Blondin et al. 2007; Blondin & Tonry 2007). The basic results from the cross-correlation analysis are listed in Table 3.

4.2. Spectral Decomposition and Host-Galaxy Subtraction

The majority of our SN spectra have substantial host-galaxy contamination (Figures 3 and 5), because of the wide slits used and relatively high redshift and small angular size of the hosts. Indeed, for late-time SN spectra and subluminous objects, the host-galaxy light coincident with the SN often dominates that of the SN itself. To study SN spectral diversity and to explore the correlation of spectral parameters with our high-quality light curves, we wish to have SN spectra with minimum contamination. Accordingly, we have attempted to quantitatively measure the SN and host contributions using PCA.

Several approaches have been developed for such spectra decomposition. One method (Madgwick et al. 2003) projects the observed spectrum onto the Karhunen–Loève (KL) transformation or PCA eigenspectra basis (Connolly et al. 1995; Folkes et al. 1996; Madgwick et al. 2002) to extract the reconstructed source (e.g., galaxy) spectrum. Other techniques use point-source deconvolution (Blondin et al. 2005) or χ^2 template-fitting techniques (Howell et al. 2002, 2005; Lidman et al. 2005; Hook et al. 2005), modeling both SN and galaxy with template libraries. However, this latter approach sometimes fails, yielding only a low-S/N detection of the SN spectrum. In such cases, it is common to resort to a cross-correlation technique similar to that used above (Matheson et al. 2005).

Here we adopt a composite PCA + template-fitting program to separate the SN spectrum from the host-galaxy light. In this procedure, each observed spectrum is modeled by a weighted combination of SN templates (identical to those used for the cross-correlations analysis) and PCA eigenspectra derived from the SDSS galaxy sample (Yip et al. 2004). The redshift is fixed to the value determined by the cross-correlation procedure above, but we allow the flux from the SN and the three dominant PCA galaxy components to vary. In addition, we optionally add a variable amount of absorption with a Galactic extinction law A_λ (standard reddening, Cardeli et al. 1989, and $R_V = 3.1$) at the host redshift. To monitor the fit we define a figure of merit (FoM) normalized by the degrees of freedom,

$$\chi^2_\nu = \sum_\lambda \frac{\left[D(\lambda) - aS(\lambda, T)10^{cA_\lambda} - \sum_{i=0}^{2} b_i G_i(\lambda)\right]^2}{\nu(\sigma(\lambda))^2}, \quad (1)$$

where D is the observed host + SN spectrum, S is the SN template spectrum at an epoch T, G_0, G_1, and G_2 are the first three major PCA eigenspectra of the SDSS galaxy sample (Yip et al. 2004), A_λ is the extinction (applied at the redshift of the SN), and σ is the 1σ error of the spectrum. Here a, b_0, b_1, b_2, and c are constants to be adjusted for the best fit in the SN spectra, host galaxy, and reddening space. The values of b_0, b_1, and b_2 indicate the galaxy type of the host (Yip et al. 2004). We neglect extinction and reddening in the Milky Way, which produces $E(B-V) < 0.1$ mag for almost all of the survey stripe. Here the ν degrees of freedom are determined as $N - m$ where N is the number of data points and m accounts for the fitting parameters and the (nearly continuous) date parameter (time from maximum light). Since the first three eigencomponents contain 98.2% of the total SDSS galaxy sample variance, the amplitudes $b_{0,1,2}$ can classify ∼99% of observed galaxies (Yip et al. 2004). These components thus provide a reasonable representation of the host spectrum, avoiding unphysical galaxy models which can be derived when many low-significance eigencomponents are included.

This procedure gives the best decomposition for a given SN template spectrum S. We can, of course, then perform this minimization for each plausible S (i.e., different SN types and ages). Figure 6 shows two examples of how the FoM χ^2_ν varies as S, type, and date change. In the upper panel of Figure 6, the large improvement near the best global maximum shows a definitive typing as an SN Ia (and a well-constrained date and decomposition). In the bottom panel of Figure 6, a standard SN Ia also provides the best fit, although an SN 1991T template is only modestly worse. Note, however, that both acceptable types show a similar well-constrained age.

If the data had Gaussian errors with the correct amplitude and the model describes the data well, we would expect χ^2_ν to approach 1, with a spread of $\Delta\chi^2_\nu \approx \nu^{-1/2}$ where $\Delta\chi^2_\nu$ stands for the difference between one solution and the best-fitted solution. In practice, however, the errors may be mis-estimated and/or the model may be wrong, giving larger χ^2_ν. One quantity that can be used under these conditions to distinguish between two models is a quality factor defined by

$$Q = \frac{\Delta\chi^2_\nu \sqrt{\nu}}{\chi^2_\nu}, \quad (2)$$

Table 3
SDSS-II SN Redshift Cross-Correlation and Type Analysis

IAUC ID[a]	SNID[b]	Epoch$_p$[c]	Epoch$_s$[d]	Type$_{SN}$[e]	z_{SN}[f]	SN Temp[g,h]	r_{SN}[i]	z_g[j]	Type$_g$[k]	r_g[l]
2005ed	722	14	17	Ia	0.087		11.9	0.0861	E/S0	17.4
2005ef	739	15	16	Ia	0.105		12.9	0.1070	E/S0	16.5
2005ei	744	11	8	Ia	0.123		4.4	0.1282	Sm/Im	4.7
2005eg	762	0	−1	Ia	0.189		7.5	0.1908	Sa	13.3
2005ex	774	14	16	Ia	0.090		10.4	0.0933	Sa	9.5
2005ex	774	22		Galaxy				0.0936	Sa	12.0
...	779	110		Galaxy				0.2377	Sbc/Sc	16.8
2005ez	1032	14	22	Ia	0.133		8.4	0.1293	Sa	10.3
2005fg	1112	10	7	Ia	0.258		4.3	0.2577	Sb	8.4
2005lb	1114	43	30	II	0.031	99em	7.2	0.0245	Sm/Im	9.2
2005fc	1119	17	17	Ia	0.298		11.6	0.2974	Sm/Im	17.0
...	1166	17	0	Ia	0.385		9.6	0.3824	E/S0	10.6
2005ff	1241	1	3	Ia	0.087		21.6			
2005fd	1253	6	4	Ia	0.262		20.6			
2005fd	1253	6		Galaxy				0.2699	Sbc/Sc	2.1
2005fd	1253	8	2	Ia	0.264		8.7			
2005fe	1316	22	20	Ia	0.216		7.2	0.2166	Sm/Im	3.1
2005fh	1371	7	12	Ia	0.130		4.1	0.1189	E/S0	8.4
...	1461	113		Galaxy				0.3407	E/S0	8.5
2005lc	1472	65	159	II	0.019	99em	15.8	0.0129	Sm/Im	7.9
...	1525	99		Galaxy				0.1072	Sa	7.0
...	1545	−2		Galaxy				0.0987	E/S0	16.4
2005fb	1580	4	9	Ia	0.184		5.8			
...	1595	11		Galaxy				0.2136	E/S0	14.3
...	1632	42		Galaxy				0.0575	Sm/Im	25.4
...	1686	11	41	Ia?	0.143		8.6	0.1364	Sm/Im	13.8
...	1688	14	14	Ia	0.357		17.5	0.3587	Sm/Im	16.6
...	1740	15		Galaxy				0.1673	E/S0	20.0
2005fj	1794	15	15	Ia	0.138		10.1	0.1426	Sm/Im	3.3
2005hl	2000	34	19	Ib	0.037	90I	3.0	0.0243	Sm/Im	17.7
2005fo	2017	3	0	Ia	0.254		8.6	0.2616	Sbc/Sc	5.1
2005fl	2030	29	37	Ia	0.237		2.1	0.2336	Sm/Im	4.5
2005fm	2031	1	2	Ia	0.154		10.0	0.1530	Sm/Im	2.1
2005fk	2053	20	3	Ic	0.266	02ap		0.2643	Sm/Im	4.4
...	2063	−4		Galaxy				0.1920	Sbc/Sc	15.9
2005fn	2102	22	16	Ia	0.095		8.2	0.0958	Sm/Im	4.2
2005fr	2165	7	8	Ia	0.288		17.7			
2005fy	2246	12	2	Ia	0.193		13.4	0.1952	Sm/Im	3.7
2005fy	2246	12	1	Ia	0.201		6.7	0.1954	Sa	3.2
2005ey	2308	8	3	Ia	0.148		10.6			
2005fp	2330	8	9	Ia	0.208		14.6	0.2132	Sb	9.9
2005fq	2366	58	44	II	0.144	99em	6.1	0.1454	Sb	5.3
...	2371	80		Galaxy				0.0508	Sm/Im	9.7
2005ft	2372	1	−4	Ia	0.183		7.7	0.1798	E/S0	3.8
2005ft	2372	3	6	Ia	0.176		6.2	0.1812	Sm/Im	5.3
2005fi	2422	4	3	Ia	0.265		11.8			
2005fu	2440	6	5	Ia	0.193		17.5			
2005fs	2533	8	6	Ia	0.340		4.6			
2005fv	2561	−3	−5	Ia	0.121		6.4			
2005fv	2561	−1	−3	Ia	0.124		5.8			
2005fv	2561	−1	−1	Ia	0.121		5.7			
2005fv	2561	2		Galaxy				0.1184	Sb	5.2
2005fw	2635	31	27	Ia	0.140		22.2	0.1433	Sbc/Sc	19.0
2005fw	2635	−1	−2	Ia	0.144		7.3	0.1434	Sm/Im	18.8
...	2661	25	5	II	0.201	99em	4.6	0.1925	Sbc/Sc	7.5
2005fa	2689	1	1	Ia	0.180		8.3			
2005hm	2744	20	51	Ib	0.040	90I	9.2	0.0350	Sm/Im	5.0
...	2746	18	2	Ia?				0.1201	Sm/Im	14.8
...	2746	18	4	Ia?				0.1201	Sb	15.0
2005fx	2789	10	2	Ia	0.295		13.6	0.2903	E/S0	10.6
...	2864	88		Galaxy				0.2441	Sa	6.8
2005fz	2916	−5	0	Ia	0.119		14.9			
2005fz	2916	−3	3	Ia	0.121		6.5			
2005fz	2916	1	7	Ia	0.122		20.8	0.1242	Sa	4.3

Table 3
(Continued)

IAUC ID[a]	SNID[b]	Epoch$_p$[c]	Epoch$_s$[d]	Type$_{SN}$[e]	z_{SN}[f]	SN Temp[g,h]	r_{SN}[i]	z_g[j]	Type$_g$[k]	r_g[l]
...	2928	91		Galaxy				0.1490	Sm/Im	5.3
...	2929	20		Galaxy				0.1192	Sa	10.8
2005go	2943	13	14	Ia	0.258		7.1	0.2654	Sm/Im	4.4
2005gp	2992	12	11	Ia	0.118		16.9	0.1268	Sb	5.9
2005gp	2992	30	31	Ia	0.128		7.2	0.1251	Sa	6.4
2005ga	3080	−5	−10	Ia	0.173		6.3	0.1750	Sa	13.4
2005ga	3080	−5	−6	Ia	0.171		9.7	0.1739	Sa	8.0
2005ga	3080	24	23	Ia	0.173		15.1	0.1742	Sb	14.0
2005gc	3087	−2	−6	Ia	0.156		10.7	0.1646	Sm/Im	11.3
2005gs	3199	8	3	Ia	0.266		4.7	0.2511	Sb	5.4
2005gh	3241	−6	6	Ia?	0.391		2.0			
2005hn	3256	17	13	Ia	0.116		6.8	0.1076	Sm/Im	4.5
2005gd	3317	−5	−4	Ia	0.163		11.6	0.1618	Sm/Im	4.2
2005ge	3331	−8	−10	Ia?	0.206		6.8			
2005gr	3377	13	4	Ia	0.243		14.0	0.2451	Sm/Im	4.0
2005gf	3451	−2	−2	Ia	0.246			0.2500	Sa	13.6
2005gg	3452	−6	−5	Ia	0.234		9.1	0.2304	Sm/Im	12.8
...	3508	87		Galaxy				0.4967	Sm/Im	8.5
...	3508	92		Galaxy				0.4967	Sm/Im	8.5
...	3535	103		Galaxy				0.3080	Sbc/Sc	5.8
2005gb	3592	−5	−5	Ia	0.089		21.0	0.0863	Sb	21.9
2005gb	3592	−1	−1	Ia	0.087		37.1			
2005gb	3592	11		Ia				0.0864	Sa	7.0
2005gi	3818	38	5	II	0.055	87a	4.5	0.0500	Sm/Im	8.5
2005ho	3901	−16		Ia				0.0626	Sm/Im	22.1
2005ho	3901	6	5	Ia	0.063		14.4	0.0636	Sm/Im	4.4
...	3959	103		Galaxy				0.1833	Sbc/Sc	9.2
...	4000	17	10	Ia	0.268		3.8	0.2786	Sm/Im	7.0
2005gt	4012	21	15	Ic	0.031	99ex	4.7	0.0252	Sm/Im	3.3
2005gw	4046	10	3	Ia	0.277		8.4			
...	4064	5		Galaxy				0.1559	E/S0	8.3
...	4236	79		Galaxy				0.3432	Sb	10.5
2005gu	4241	21	14	Ia	0.3320		5.5	0.3320	Sm/Im	4.2
...	4281	2		Galaxy				0.2132	E/S0	5.8
...	4307	81		Galaxy				0.2720	Sb	3.2
...	4311	77		Galaxy				0.2953	Sa	10.4
2005gj[m]	4524	−14		Ia				0.0618	Sbc/Sc	11.0
2005gj	4524	−12		Ia				0.0622	Sm/Im	12.8
2005gj	4524	−8		Ia				0.0618	Sm/Im	9.8
2005gj	4524	−3	4	Ia	0.064		2.4	0.0618	Sbc/Sc	8.8
2005gj	4524	7		Ia				0.0613	Sbc/Sc	16.4
2005gj	4524	10		Ia				0.0618	Sbc/Sc	14.4
2005gj	4524	18		Ia				0.0616	Sbc/Sc	12.3
2005gj	4524	26		Ia						
2005gj	4524	28		Ia						
2005gj	4524	28		Ia				0.0620	Sbc/Sc	10.8
2005gj	4524	42		Ia				0.0619	Sbc/Sc	11.5
2005gj	4524	44	42	Ia	0.067		7.2	0.0616	Sbc/Sc	12.2
2005gj	4524	54	42	Ia	0.068		8.1	0.0615	Sbc/Sc	11.3
2005gj	4524	71	45	Ia	0.070		6.0	0.0616	Sbc/Sc	17.0
2005gv	4577	9	1	Ia?	0.363					
...	4676	77		Galaxy				0.2446	Sa	6.6
2005gy	4679	2	−2	Ia	0.338		3.1	0.3324	Sm/Im	4.4
2005gx	5103	−5	7	Ia	0.146		4.9			
2005gq	5183	13	−4	Ia	0.382		3.5	0.3898	Sb	5.6
2005hp	5350	8	3	Ia	0.174		6.1	0.1754	Sbc/Sc	13.5
...	5378	76		Galaxy				0.2511	E/S0	3.4
2005hs	5391	13	14	Ia	0.295		7.5	0.3009	Sm/Im	4.2
2005hr	5395	4	1	Ia	0.115		4.4	0.1170	Sbc/Sc	5.5
2005hu	5533	6	5	Ia	0.224		37.3	0.2197	Sm/Im	28.4
2005hx	5549	0	1	Ia	0.121		12.9			
2005hy	5550	−3	−1	Ia	0.154		5.0	0.1562	Sb	7.6
2005hw	5588	10	8	Ia	0.407		3.1	0.4102	E/S0	8.2
2005hv	5635	5	3	Ia	0.181		10.4	0.1795	Sm/Im	4.1

Table 3
(Continued)

IAUC ID[a]	SNID[b]	Epoch$_p$[c]	Epoch$_s$[d]	Type$_{SN}$[e]	z_{SN}[f]	SN Temp[g,h]	r_{SN}[i]	z_g[j]	Type$_g$[k]	r_g[l]
...	5673	11		Galaxy				0.3793	E/S0	12.1
2005ia	5717	9	3	Ia	0.251		15.9	0.2517	Sm/Im	6.7
2005jz	5736	17	14	Ia	0.253		8.0			
2005ib	5737	9	3	Ia	0.393		18.2	0.3930	Sm/Im	8.8
2005hz	5751	2	0	Ia	0.133		3.9	0.1301	Sbc/Sc	4.2
2005hz	5751	36	35	Ia	0.133		7.0	0.1300	Sb	6.8
2005hq	5821	16	18	Ia?	0.423		2.5			
2005hq	5821	18	14	Ia?	0.423		2.0	0.4008	Sbc/Sc	3.8
2005ic	5844	15	2	Ia	0.314		13.1	0.3108	Sm/Im	4.1
2005is	5916	7	4	Ia	0.177		2.4	0.1724	Sb	6.5
2005is	5916	12	13	Ia	0.177		6.2	0.1740	Sb	5.3
2005hc	5944	−3	−4	Ia	0.045		19.3			
2005hc	5944	−1	1	Ia	0.044		22.9			
2005hc	5944	34	34	Ia	0.046		16.1	0.0453	E/S0	6.8
2005ie	5957	6	4	Ia	0.286		14.9	0.2796	Sm/Im	15.0
...	5963	64		Galaxy				0.2356	Sbc/Sc	11.5
2005it	5966	19	17	Ia	0.301		3.3	0.3082	Sm/Im	9.0
...	5993	78		Galaxy				0.3767	Sa	11.5
2005ht	5994	4	1	Ia	0.187		11.5			
2005if	6057	3	7	Ia	0.067		1.7	0.0675	Sm/Im	5.4
2005if	6057	37	35	Ia	0.070		9.2	0.0664	Sm/Im	11.5
2005ka	6100	21	13	Ia	0.316		4.5	0.3177	Sm/Im	9.2
2005ih	6108	0	2	Ia	0.262		11.5	0.2595	Sm/Im	4.4
2005iw	6127	9	2	Ia	0.280		5.1			
2005iv	6137	11	−1	Ia	0.311		3.5	0.3001	Sbc/Sc	4.0
2005jy	6192	10	6	Ia	0.272		18.2	0.2720	Sm/Im	12.5
2005ig	6196	7	1	Ia	0.279		11.8	0.2807	E/S0	9.9
2005ii	6249	0	−4	Ia	0.290		13.7	0.2944	Sm/Im	11.0
2005js	6295	17	18	Iapec	0.082	1991bg	8.5	0.0791	E/S0	12.5
2005jk	6304	10		Galaxy				0.1903	Sm/Im	7.7
2005jk	6304	9	10	Ia	0.183		23.0			
2005ix	6315	1	−5	Ia	0.263		6.0	0.2670	Sm/Im	5.1
2005ix	6315	5	2	Ia	0.255		15.6			
2005ij	6406	−6	−9	Ia	0.122		3.6	0.1231	Sb	3.4
2005ij	6406	27	25	Ia	0.123		17.7	0.1227	Sb	3.3
2005id	6422	1	2	Ia	0.184		7.9			
...	6471	3	16	II	0.210	99em	5.8	0.2016	Sbc/Sc	5.2
2005hj[n]	6558			Ia						
2005jd	6649	4	6	Ia	0.314		3.8			
2005jd	6649	0	−5	Ia	0.330		3.8			
...	6696	5		Ia?				0.2379	Sm/Im	8.5
2005ik	6699	−1	2	Ia	0.312		14.0	0.3106	Sb	8.8
2005ik	6699	7	2	Ia	0.313		19.5			
...	6714	54		Galaxy				0.4137	Sm/Im	12.3
2005iu	6773	−5	−4	Ia	0.088		6.2	0.0904	Sa	5.8
2005iy	6777	17	2	Ia	0.404		3.0	0.4043	Sb	2.9
2005iy	6777	20	8	Ia	0.394		2.0			
2005iz	6780	12	13	Ia	0.202		8.0			
2005jf	6852	−3		Ia?				0.3006	Sa	8.6
2005ja	6924	5	0	Ia	0.328		8.2			
2005jc	6933	−1	0	Ia	0.214		6.7			
2005jc	6933	2	1	Ia	0.213		15.8			
2005jl	6936	0	0	Ia	0.186		19.8	0.1810	Sm/Im	3.3
2005je	6962	13	13	Ia?	0.097		2.1	0.0930	Sa	7.5
...	6968	12	13	Ia?	0.119		2.8	0.0980	Sb	7.9
...	7017	318	405	Ia	0.271	2005gj	13.8	0.2684	Sm/Im	15.7
...	7099	0		Galaxy				0.2186	Sa	5.4
...	7102	7		Galaxy				0.1965	Sm/Im	3.2
2005jg	7143	1	−1	Ia	0.304		6.6			
2005jh	7147	2	2	Ia	0.109		12.1	0.1099	E/S0	4.7
2005jh	7147	−1	1	Ia	0.109		6.2	0.1100	E/S0	4.0
2005jm	7243	−5	−4	Ia	0.197		23.7	0.2037	Sm/Im	10.1
2005kn	7335	8	14	Ia?	0.197		1.4			
2005jb	7426	−7	0	Ia?	0.384		2.2			

Table 3
(Continued)

IAUC ID[a]	SNID[b]	Epoch$_p$[c]	Epoch$_s$[d]	Type$_{SN}$[e]	z_{SN}[f]	SN Temp[g,h]	r_{SN}[i]	z_g[j]	Type$_g$[k]	r_g[l]
...	7444	44		Galaxy				0.2499	Sb	6.7
2005jx	7460	7	8	Ia?	0.218		2.1	0.2103	Sb	3.3
2005ji	7473	1	2	Ia	0.221		5.1			
2005ji	7473	2	2	Ia	0.216		18.3			
2005jn	7475	5	2	Ia	0.322		8.5			
2005jn	7475	5	6	Ia	0.326		5.7			
2005jo	7512	−1	2	Ia	0.219		11.6			
...	7647	49		Galaxy				0.3854	Sm/Im	11.0
2005jw	7779	8	7	Ia	0.374		4.2	0.3812	Sbc/Sc	3.0
2005jp	7847	0	−3	Ia	0.209		10.9	0.2124	Sb	3.2
2005ir	7876	−9	−5	Ia	0.062		8.3	0.0762	Sb	24.7
2005ir	7876	−5	−3	Ia	0.070		7.4	0.0761	Sbc/Sc	16.1
...	7922	0		Galaxy				0.1822	Sb	16.9
2005jj	7947	7	6	Ia?	0.368		6.1			
2005jv	8030	8	6	Ia	0.422		5.7			
2005ju	8046	−2	−4	Ia	0.251		9.4	0.2593	E/S0	11.6
2005hk[o]	8151	−7		Ia						
2005hk	8151	−6		Ia				0.0124	Sm/Im	21.8
2005hk	8151	−5		Ia				0.0125	Sm/Im	3.8
2005hk	8151	−1		Ia						
2005hk	8151	1		Ia						
2005hk	8151	−7		Ia						
2005hk	8151	3		Ia						
2005hk	8151	26		Ia						
2005ko	8213	13	18	Ia	0.184		9.3	0.1847	Sbc/Sc	3.5
2005mi	8495	23	22	Ia	0.212		4.6	0.2144	Sb	10.1
2005jt	8598	5	20	Ia	0.356		3.3	0.3606	Sm/Im	7.7
2005jr	8679	−3		II				0.2944	Sm/Im	6.0
2005mh	8707	28	16	Ia?	0.400		3.5	0.3951	Sb	3.2
2005kp	8719	−6	−6	Ia	0.113		9.1	0.1163	Sm/Im	10.6
...	8742	49		Galaxy				0.2141	Sm/Im	17.2
2005ld	8921	6	6	Ia	0.149		6.9	0.1454	Sm/Im	5.6
2005le	9032	14	14	Ia	0.253		14.8	0.2540	Sm/Im	14.3
2005kq	9045	15	15	Ia	0.393		3.7	0.3895	Sm/Im	10.0
2005kr	9118	7	3	Ic	0.124	02ap	1.5	0.1338	Sm/Im	13.1
2005lg	9207	15	15	Ia	0.345		23.0	0.3500	Sb	7.1
2005ks	9273	8	19	Ic	0.102	02ap	2.8	0.0989	Sm/Im	23.5
2005li	9457	11	14	Ia	0.254		4.5	0.2569	Sa	5.4
2005lh	9467	18	16	Ia	0.218		8.3	0.2184	Sa	8.8
...	9954	40		Galaxy				0.2277	Sm/Im	7.4
2005kt	10028	26	1	Ia	0.063		5.9	0.0662	E/S0	5.9
...	10045	11		Galaxy				0.1147	Sb	9.2
2005lj	10096	7	7	Ia	0.075		4.5	0.0774	Sbc/Sc	16.1
...	10106	39	37	Ia?	0.155		3.5	0.1472	Sb	6.0
2005mk	10297	16	10	II	0.151	99em	6.1	0.1477	Sb	4.7
2005kb	10367	42	7	II	0.015	99em	19.8	0.0155	Sbc/Sc	3.2
2005lk	10434	1	2	Ia	0.109		10.1	0.1040	E/S0	10.6
2005ll	10449	6	2	Ia	0.244		13.1			
2005lf	10550	13	11	Ia	0.302		13.0	0.3001	Sm/Im	26.0
2005ku	10805	−2	1	Ia	0.039		17.2	0.0456	Sm/Im	11.1
2005lm	10907	4	10	II	0.090	99em	4.4	0.0842	Sm/Im	18.7
...	10915	42		Galaxy				0.2244	Sm/Im	3.9
...	10928	9		Galaxy				0.0815	Sbc/Sc	22.3
...	10976	6		Galaxy				0.0971	Sa	4.6
2005mj	11017	3		II						
2005ml	11067	7	8	Ia	0.114		5.6			
2005mm	11206	19	7	Ia	0.382		5.4	0.3819	Sa	5.2
2005ln	11300	−1	0	Ia	0.128		9.2	0.1370	Sm/Im	4.6
2005mo	11320	22	13	Ia	0.278		1.3	0.2743	Sm/Im	5.5
2005mn	11332	2	19	Ib	0.054	90I	5.8	0.0469	Sb	10.1
2005mn	11332	6	19	Ib	0.051	90I	7.8	0.0469	Sm/Im	10.0
2005mn	11332	8	19	Ib	0.054	90I	12.6	0.0473	Sb	11.1
2005mn	11332	64	39	Ib	0.058	90I	4.5	0.0480	Sb	3.8
2005lo	11452	16	8	Ia	0.299		3.6			

Table 3
(Continued)

IAUC ID[a]	SNID[b]	Epoch$_p$[c]	Epoch$_s$[d]	Type$_{SN}$[e]	z_{SN}[f]	SN Temp[g,h]	r_{SN}[i]	z_g[j]	Type$_g$[k]	r_g[l]
2005lq	11557	−1	−2	Ia	0.380		5.6			
2005mp	11650	−1	−1	Ia	0.273		10.9			
2005lp	11864	16	3	Ia	0.303		5.2			
2005mq	12136	7	7	Ia	0.350		5.9			

Notes.
[a] Official IAU name, when assigned.
[b] SDSS Internal SN ID.
[c] Spectrum day (in observer frame) relative to epoch of maximum brightness from the photometric typing.
[d] Spectrum day (in observer frame) relative to epoch of maximum brightness from the spectroscopic cross-correlation analysis.
[e] Best-fitted type of the SNe. "Ia?" indicates a best match to an SN Ia template, although some features are not detected. "II?" indicates a general match to the SN II template, although expected SN II features are not all detected. "Ia-pec" indicates peculiar SN Ia.
[f] Redshift measured from cross-correlation against SN templates. This value has been corrected for the systematic offset 0.003. The expected redshift error is 0.005.
[g] Template spectrum providing the best match to the observed spectrum. If blank, then the best-fitted template belongs to the Nugent SN Ia set.
[h] SN templates from Pun et al. (1995), Turatto et al. (1996), Hamuy et al. (2002), Gal-Yam et al. (2002), Leonard et al. (2002), Elmhamdi et al. (2004), and Nugent et al. (2002).
[i] r value of the rvsao.xcsao comparison with SN templates. $r_{SN} > 3$ is a criterion for a "good" fit. See text for details.
[j] Redshift from cross-correlation against galaxy templates. The expected redshift error is 0.0005.
[k] Best-fit type of the host galaxy.
[l] r value for rvsao.xcsao correlation against host-galaxy templates. $r_g > 3$ is a criterion for a "good" fit. See text for details.
[m] Initially identified as a normal SN Ia by cross-correlation analysis. Later, determined to be a peculiar SN Ia (SN 2002ic-like) based on detailed spectroscopic analysis.
[n] This SN was confirmed by another group using the HET (CBET 266; Quimby et al. 2007). The spectrum is not available.
[o] Initially identified as a normal SN Ia by cross-correlation analysis. Later, determined to be a peculiar SN Ia (SN 1991T-like), based on detailed spectroscopic analysis.

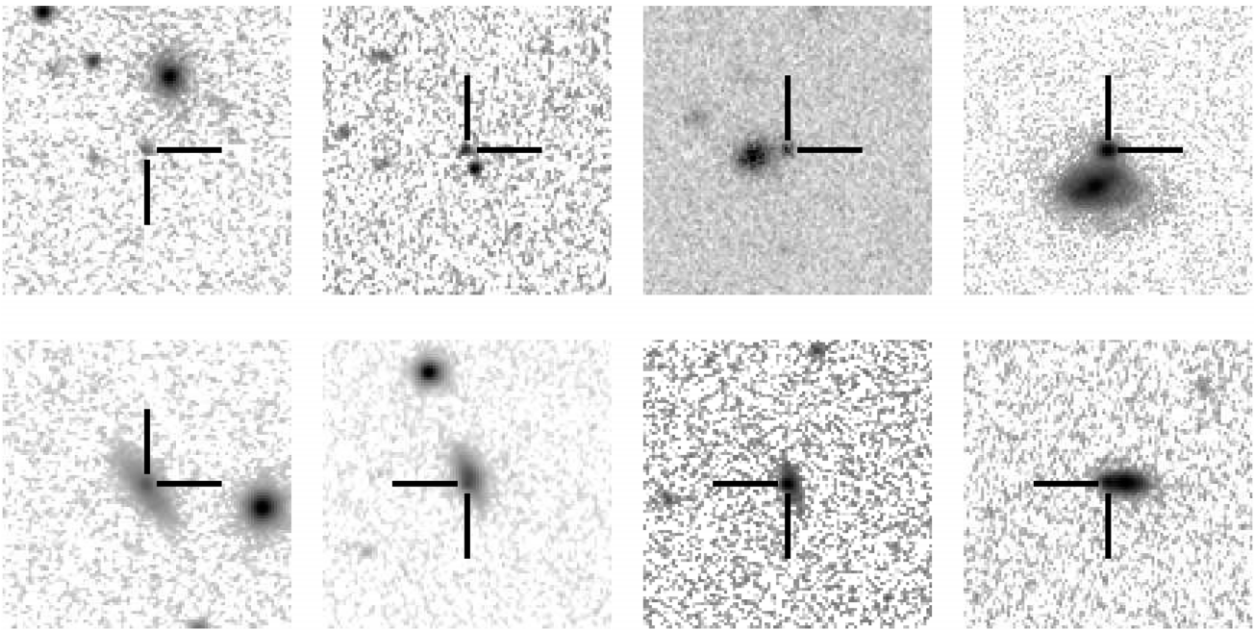

Figure 5. This panel shows images of "clean" (top row) and "heavily contaminated" (bottom row) SNe. The tick marks indicate the location of the SN.

where the χ^2_ν value for the best-fitted model is inserted in the denominator to compensate for incorrect error estimates. Large $\Delta\chi^2_\nu$ yields large Q values and thus more significant discrimination between the models. In fact, even when the models are not correct or equivalently the data suffer uncorrected systematic bias, a large value of Q ($\gtrsim$1) can indicate a significant discrimination between two models.

Unfortunately, we find that we do not always satisfy this criterion ($Q \gtrsim 1$), even when visual inspection indicates a clear-type assignment, so our PCA analysis does not always definitively type the SN. While it does indeed confirm the clear SN identifications, and while the "best" type (albeit at small $\Delta\chi^2_\nu/\chi^2_\nu$) is often that selected by hand, there are some disagreements with the types selected manually from the r

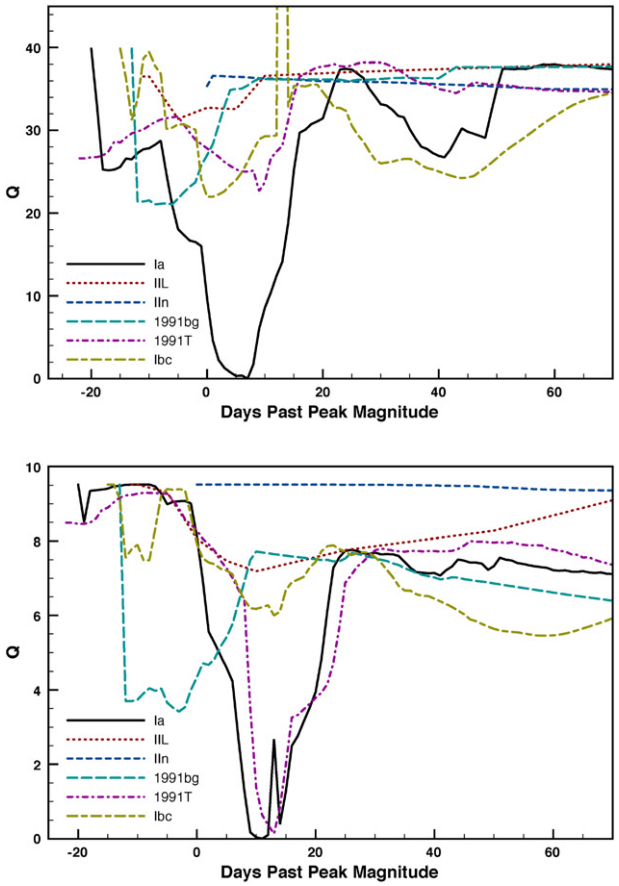

Figure 6. Two panels showing χ^2_ν fitting results to various SN templates as a function of age. The object in the upper panel, with $\nu = 943$ degrees of freedom, is classified as an SN Ia at high confidence, since the quality factor $Q = \Delta\chi^2_\nu\sqrt{\nu}/\chi^2_\nu$ of the next-best-type solution is $\gg 1$. The lower panel, with $\nu = 918$ degrees of freedom, has a preferred but not definitive SN Ia classification, with $Q \ll 1$. The photometric ages for these two objects are 5 d and 16 d after B-band maximum respectively; the spectroscopic age estimates are consistent with this value.

(A color version of this figure is available in the online journal)

values of the cross-correlation analysis. At least for our typical data quality, it seems that PCA analysis does not provide a reliable automatic classifier for low-S/N spectra. In particular, the $\Delta\chi^2_\nu/\chi^2_\nu$ analysis has difficulty in distinguishing between SN Ia subtypes. Thus, in ambiguous cases, we defer to the typing from the cross-correlation analysis. However, even in these cases, the PCA analysis is valuable, as it provides a quantitative estimate of the galaxy/SN decomposition.

As noted above, we can, in principle, independently measure the absorption from the spectrum reddening. However, when we allow c, the coefficient that characterizes the amount of extinction and reddening, to range freely, the value at χ^2_ν minimum is often higher than that determined from the light-curve analysis. One difference is that the light-curve analysis includes an exponential prior (favoring low A_V values), while we do not impose a prior. However, we believe that the limited accuracy of our relative spectrophotometry prevents us from making useful reddening measurements. This is seen in the large dispersion of the fit values. Also it may be problematic that our assumed extinction law, which corresponds to the standard Galactic $R_V = 3.1$, may not apply to SNe Ia host environments. Indeed widely values have been estimated for R_V (e.g. Branch & Tammann 1992; 1.55, Krisciunas et al. 2006; 2.5, Knop et al. 2003, Altavilla et al. 2004, etc). Accordingly, for our final decomposition we fix the value of the extinction to that obtained from the light-curve analysis. The redshift and spectral identification are not very sensitive to the value of A_V to within their uncertainties.

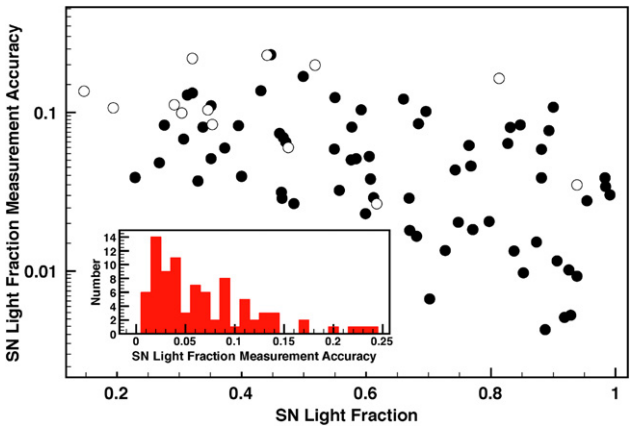

Figure 7. The accuracy of the SN component measurement (defined as the statistical error of SN light flux divided by the fraction of SN light flux) plotted versus SN fraction. "Type Ia?" (empty circles) tend to have relatively low accuracy. In most cases, the SN fraction is measured to within <10%.

(A color version of this figure is available in the online journal)

Thus, adopting the z and SN type from the cross-correlation analysis and the extinction from the light-curve fitting, we can use the PCA decomposition to obtain a model galaxy spectrum and a fraction of SN light together with statistical errors (two-sided, asymmetric error bars with a 1σ confidence level). The accuracy of such measurement versus the magnitude of the fraction is shown in Figure 7. The relatively low-significance points include SNe of the "Ia?" class, for which the characteristic lines were not measured with high significance, but the general spectral shape was best fitted by an SN Ia template.

In general, the typing from cross-correlation analysis and PCA decomposition were consistent. The epochs determined from both analysis mostly agree within ~5 days and are close to those estimated from photometry analysis (see Figure 8). Approximately 80% of the galaxy types determined from the PCA analyses are consistent with the cross-correlation results. No prior is assumed except for the physical constraints on the parameters ($a > 0$, constraints on the b_0, b_1, and b_2 to make sure the constructed galaxy type is physically plausible). The fit values are listed in Table 4. Figure 9 presents typical synthetic SN/host spectra, with relative amplitudes determined from the PCA analysis.

5. CONCLUSION AND FUTURE WORK

We have presented the follow-up spectroscopy for the fall 2005 season of the SDSS-II SN Survey. A semi-quantitative procedure of SN identification is developed, based on cross-correlation techniques. The rvsao.xcsao r value and the overlap of template and data in wavelength space are useful guides to the quality of the fit. Nevertheless, a fair amount of human judgment is required to flag solutions associated with false local minima for low-S/N spectra. Using this procedure, we have determined accurate redshifts from both SN spectra and host spectra within $\delta z_{\rm SN} \approx 0.005$ and $\delta z_{\rm gal} \approx 0.0005$, respectively. The typical uncertainty in phase is ~3 d.

Table 4
SDSS-II SNe Spectral Decomposition and Host Analysis Results

SNID[a]	Tel[b]	Epoch_p[c]	SN_s[d]	Epoch_{sh}[e]	Host_{sh}[f]	SN Frac[g]	χ^{2h}_ν	Q[i]
1112	HET	10	Ia/1999ac	9	Sb	0.307 ± 0.021	1.88	−1
1253	HET	5	Ia/1999ac	7	Sb	0.669 ± 0.019	2.14	2.6
2017	HET	3	Ia/1991T	−5	Sbc/Sc	0.351 ± 0.018	1.96	−0.5
2030	HET	29	Ia/1990I	44	Sbc/Sc	0.431 ± 0.059	4.93	−0.1
2533	HET	8	Ia/1991T	2	E/S0	0.584 ± 0.03	0.88	4.4
3199	HET	8	Ia/1997cy	11	Sbc/Sc	0.499 ± 0.084	2.12	−0.6
3377	HET	13	Ia/1999ac	8	Sm/Im	0.743 ± 0.032	2.54	−0.2
4000	HET	17	Ia/1997br	14	Sbc/Sc	0.395 ± 0.033	1.39	0
4046	HET	10	Ia/Ibc	15	E/S0	0.684 ± 0.058	2.62	−6.3
4241	HET	21	Ia/1999aa	14	Sm/Im	0.66 ± 0.08	1.12	0.1
4577	HET	9	Ia?/1991T	7	Sb	0.346 ± 0.036	1.45	0.3
4679	HET	2	Ia/1991T	2	Sbc/Sc	0.605 ± 0.032	1.17	3
5183	HET	13	Ia/1999aa	2	Sb	0.471 ± 0.031	0.69	1.3
5588	HET	10	Ia/Ibc	8	E/S0	0.321 ± 0.043	0.37	0.3
5736	HET	17	Ia/2000cx	14	Unknown	0.984 ± 0.034	1.73	1.5
5966	HET	19	Ia/1997br	19	Sbc/Sc	0.592 ± 0.061	0.59	−0.4
6100	HET	21	Ia/1997br	10	Sbc/Sc	0.467 ± 0.032	0.86	−0.8
6127	HET	9	Ia/Ibc	−1	Sb	0.313 ± 0.04	1.2	1.1
6192	HET	10	Ia/1999ac	8	E/S0	0.768 ± 0.035	1.25	−0.7
6649	HET	4	Ia/1999ac	2	Unknown	0.991 ± 0.03	1.09	13.9
6777	HET	17	Ia/1997br	7	Sm/Im	0.55 ± 0.068	0.43	−0.4
6777	HET	20	Ia/1999ac	6	Unknown	0.9 ± 0.097	0.53	−0.9
6780	HET	12	Ia/1991T	9	Unknown	0.847 ± 0.071	2.32	−1.7
6924	HET	5	Ia/1999ac	6	Unknown	0.954 ± 0.027	0.88	8.7
7143	HET	1	Ia/1999aa	6	E/S0	0.576 ± 0.029	1.14	3.8
7475	HET	5	Ia/1991T	2	Sm/Im	0.881 ± 0.034	2.46	1.8
7779	HET	8	Ia/1999ac	4	E/S0	0.881 ± 0.052	1.08	2.8
8030	HET	8	Ia/1999ac	6	Sa	0.893 ± 0.069	1.09	1.9
8046	HET	−2	Ia /Ibc	−10	E/S0	0.33 ± 0.012	1.6	0.2
8213	HET	13	Ia/1997br	20	E/S0	0.4 ± 0.016	2.75	−1
8495	HET	23	Ia/1991T	15	Sb	0.276 ± 0.023	3.17	−0.4
8598	HET	5	Ia/1991T	9	Sm/Im	0.696 ± 0.071	1.36	0.3
9045	HET	15	Ia/1991T	9	Sm/Im	0.549 ± 0.032	0.65	1.3
9457	HET	11	Ia/1993J	−5	Sb	0.351 ± 0.039	1.35	0.1
9467	HET	18	Ia/1999aa	16	Sb	0.338 ± 0.027	4.07	0.5
11206	HET	19	Ia/1998bw	12	Sb	0.373 ± 0.022	0.17	1.2
11320	HET	22	Ia/1997cy	12	Sbc/Sc	0.447 ± 0.103	1.2	−0.6
11452	HET	16	Ia/1991T	11	Sm/Im	0.827 ± 0.053	1.18	0.1
11557	HET	−1	Ia/1999aa	6	Sb	0.765 ± 0.047	0.63	2.1
11864	HET	16	Ia/1991T	9	Sbc/Sc	0.577 ± 0.047	0.94	−1.1
12136	HET	7	Ia/1999ac	12	Unknown	0.983 ± 0.038	0.67	1.5
1166	Subaru	17	Ia/1997br	8	Sa	0.607 ± 0.023	1.03	−3.1
1688	Subaru	14	Ia/1999ac	9	Sb	0.464 ± 0.015	1.36	−1.1
2165	Subaru	7	Ia/1999ac	7	E/S0	0.928 ± 0.005	1.47	0.7
2330	Subaru	8	Ia/1999ac	8	E/S0	0.702 ± 0.005	1.85	6.5
2422	Subaru	4	Ia/1999ac	1	Sbc/Sc	0.727 ± 0.01	2.21	17.5
2635	Subaru	31	Ia/1999aa	29	E/S0	0.837 ± 0.011	1.7	−3.2
2789	Subaru	10	Ia/1999ac	5	E/S0	0.938 ± 0.009	0.91	3.8
2992	Subaru	30	Ia/1999aa	30	E/S0	0.484 ± 0.013	1.71	−2.8
3080	Subaru	24	Ia/1999aa	16	E/S0	0.505 ± 0.007	2.95	−18.7
3451	Subaru	−2	Ia/1991T	1	Sb	0.595 ± 0.011	1.29	6.3
3452	Subaru	−6	Ia/1991T	−5	Sbc/Sc	0.617 ± 0.011	1.22	6.8
5391	Subaru	13	Ia/1997br	13	E/S0	0.906 ± 0.011	1.09	−1.2
5533	Subaru	6	Ia/1999ac	7	E/S0	0.887 ± 0.004	2.23	−1.2
5717	Subaru	9	Ia/1999ac	5	Sb	0.67 ± 0.012	3.76	7
5737	Subaru	9	Ia/1999ac	7	Sb	0.599 ± 0.014	1.32	3.2
5751	Subaru	36	Ia/1999ac	40	E/S0	0.229 ± 0.009	10.84	−3.2
5844	Subaru	15	Ia/1999ac	6	E/S0	0.873 ± 0.013	1.54	8.3
5944	Subaru	34	Ia/1999ac	31	E/S0	0.852 ± 0.008	3.48	−14
5957	Subaru	6	Ia/1999ac	6	E/S0	0.925 ± 0.009	1.03	−1.2
6057	Subaru	37	Ia/1999ac	30	Sm/Im	0.465 ± 0.013	37.92	−2.8
6108	Subaru	0	Ia/1999ac	3	Sa	0.681 ± 0.011	1.65	6.5
6196	Subaru	7	Ia/1999ac	0	E/S0	0.364 ± 0.006	1.65	13.4
6249	Subaru	0	Ia/Ibc	−1	Sbc/Sc	0.613 ± 0.009	1.63	25.6

Table 4
(Continued)

SNID[a]	Tel[b]	Epoch$_p$[c]	SN$_s$[d]	Epoch$_{sh}$[e]	Host$_{sh}$[f]	SN Frac[g]	χ_ν^{2h}	Q[i]
6406	Subaru	27	Ia/1999aa	30	E/S0	0.484 ± 0.005	5.55	7.1
6699	Subaru	7	Ia/1999ac	2	E/S0	0.771 ± 0.014	0.84	13.9
9032	Subaru	14	Ia/1999ac	13	E/S0	0.918 ± 0.005	1.56	10.9
9207	Subaru	15	Ia/1999ac	9	E/S0	0.612 ± 0.018	1.24	−2.1
10449	Subaru	6	Ia/1999ac	6	Sa	0.748 ± 0.015	1.44	7.1
10550	Subaru	13	Ia/1999ac	9	E/S0	0.797 ± 0.016	1.28	3.4
2053	HET	20	Ic(02ap)/1997br	3	E/S0	0.732 ± 0.038	0.81	15
2366	HET	58	II(99em)/2n	38	Sb	0.137 ± 0.03	0.57	30.6
2943	HET	13	Ia/1997br	14	Sbc/Sc	0.831 ± 0.067	1.28	−1.3
5350	HET	8	Ia/1997br	−5	Sa	0.268 ± 0.013	3.11	−1.4
5821	HET	18	Ia?/Ibc	−5	E/S0	0.292 ± 0.033	0.63	−0.6
5821	HET	16	Ia?/1991T	8	Sbc/Sc	0.321 ± 0.07	0.63	−0.6
6137	HET	11	Ia/1999ac	14	Sbc/Sc	0.461 ± 0.034	0.94	0.7
6315	HET	1	Ia /Ibc	−4	Sbc/Sc	0.557 ± 0.018	2.07	10.4
6696	HET	5	Ia?/1998bw	−5	Sbc/Sc	0.304 ± 0.03	1.96	−4.5
6852	HET	−3	Ia?/1991T	1	Sbc/Sc	0.194 ± 0.021	1.12	−2.7
7335	HET	8	Ia?/1991T	45	Unknown	0.813 ± 0.133	1.63	−1.3
7426	HET	−7	Ia?/1991T	2	Sbc/Sc	0.441 ± 0.101	0.95	−1.5
7460	HET	7	Ia?/IIl	−5	E/S0	0.353 ± 0.03	2.67	0.1
7947	HET	7	Ia?/1998bw	2	Sbc/Sc	0.475 ± 0.029	1.26	0
8707	HET	28	Ia?/IIl	15	Sm/Im	0.518 ± 0.103	0.46	−0.6
9118	HET	7	Ic(02ap)/hyper	−4	Sbc/Sc	0.413 ± 0.024	4.85	4.4
9273	HET	8	Ic(02ap)/hyper	−5	Sb	0.122 ± 0.017	7.34	−0.1
10106	HET	39	Ia?/1991T	30	Sa	0.147 ± 0.02	0.95	−1.3
10297	HET	16	II(99em)/1998bw	38	Sbc/Sc	0.057 ± 0.018	0.98	23.1
11332	HET	2	Ibc/hyper	12	Sa	0.17 ± 0.017	8.96	−2.7
11332	HET	8	Ibc/hyper	22	E/S0	0.323 ± 0.015	12.89	−0.4
11332	HET	64	Ibc/IIn	1	Sa	0.113 ± 0.012	6.37	−0.2
11650	HET	−1	Ia/1999ac	13	Unknown	0.938 ± 0.033	1.21	−1.2
1686	Subaru	11	Ia?/1991T	28	E/S0	0.617 ± 0.016	0.95	−1.3
2661	Subaru	25	II(99em)/IIl	6	Sa	0.205 ± 0.007	1.07	1.8
6471	Subaru	3	II(99em)/Ibc	5	Sbc/Sc	0.413 ± 0.012	1.07	−0.2

Notes.
[a] SDSS internal SN ID.
[b] Spectroscopic follow-up telescope.
[c] Observation date of the SN relative to B-band maximum brightness estimated from light-curve fits.
[d] The best and second-best SN type from cross-correlation analysis. "Ia?" indicates best fit to an SN Ia template, but a reasonable fit to the next-best type.
[e] Age of the SN relative to B-band maximum brightness estimated from spectrum decomposition.
[f] Host-galaxy type ID from spectral decomposition. Unknown indicates too little host light for type ID.
[g] Estimate of the SN light fraction in the observed spectrum, with statistical error (the maximum value of the asymmetric errors obtained from the PCA code).
[h] Reduced χ^2 value.
[i] Quality factor $Q = \frac{\Delta\chi_\nu^2\sqrt{\nu}}{\chi_\nu^2}$, which estimates the significance of the χ^2 differentiation between the best two SN types. Negative values indicate a selected type differing from that determined by the cross-correlation analysis.
[j] SNe above the line have extinction estimates from MCLS2k2 analysis (Jha et al. 2007). Those below the line have A_V from light-curve fitting using the frame difference photometry.

We have also described our efforts to quantify host-galaxy contamination using a combined χ^2 fitting and PCA analysis, which provides an efficient way to give useful decompositions into SN and host-galaxy spectra with <10% accuracy, given known SN types from cross-correlation analysis and host-galaxy extinction estimated from the multi-band light curves. Typically, when the spectrum contains more than 60% host-galaxy light, the host type is well constrained. Both spectroscopic analyses show good agreement in estimating the photometric epoch.

Using our quantitative measurement of the SN light fraction, we can make galaxy-subtracted SN spectra with estimates of the residual galaxy contamination. With a >50% larger yield from the second season, 2006, and an anticipated large number of SNe in the third and final seasons, the classified and host-subtracted spectra will provide a large and uniform data set with which to study SN spectral variations and evolution. We expect that this will help substantially in calibrating our use of SNe as distance indicators and will allow improved calibration of the SDSS-II and future larger (e.g., the Panoramic Survey Telescope and Rapid Response System, the Dark Energy Survey, the Large Survey Telescope, and the Joint Dark Energy Mission) SN samples.

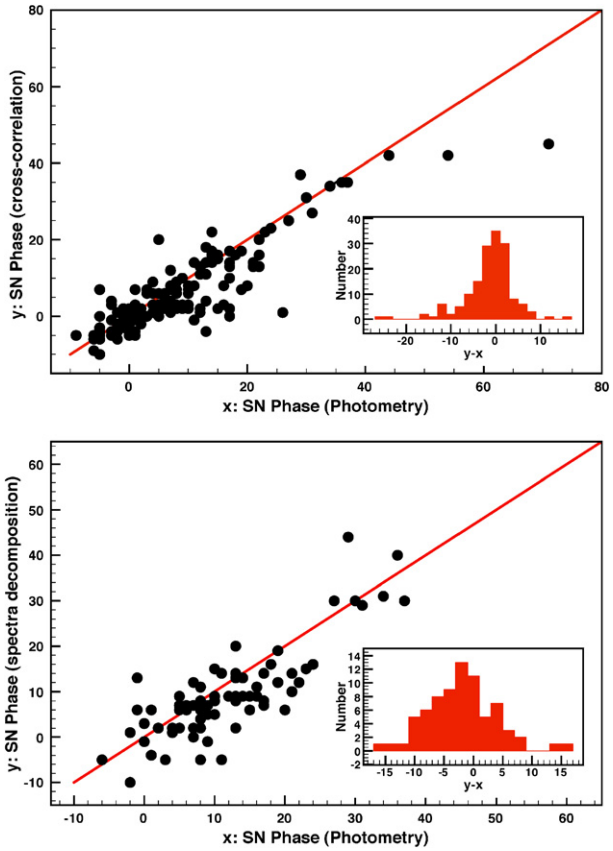

Figure 8. Two panels comparing different-epoch measurements of confirmed SNe Ia. The upper panel shows the SN phase (days past peak B-band magnitude) measured from cross-correlation analysis of the spectra against the photometric phase. The lower plot shows the SN phase measured from the PCA + template-fitting program against the photometric phase. The insets show histograms of the scatter between the two epoch measurements, with y being the phase determined from either cross-correlation analysis or the spectra decomposition analysis and x being the phase determined from light-curve fitting.

(A color version of this figure is available in the online journal)

Funding for the SDSS and SDSS-II has been provided by the Alfred P. Sloan Foundation, the Participating Institutions, the National Science Foundation (NSF), the U.S. Department of Energy, the National Aeronautics and Space Administration (NASA), the Japanese Monbukagakusho, the Max Planck Society, and the Higher Education Funding Council for England. The SDSS Web Site is http://www.sdss.org/.

The SDSS is managed by the ARC for the Participating Institutions. The Participating Institutions are the American Museum of Natural History, Astrophysical Institute Potsdam, University of Basel, University of Cambridge, Case Western Reserve University, University of Chicago, Drexel University, Fermilab, the Institute for Advanced Study, the Japan Participation Group, Johns Hopkins University, the Joint Institute for Nuclear Astrophysics, the Kavli Institute for Particle Astrophysics and Cosmology, the Korean Scientist Group, the Chinese Academy of Sciences (LAMOST), Los Alamos National Laboratory, the Max Planck Institute for Astronomy (MPIA), the Max Planck Institute for Astrophysics (MPA), New Mexico State University, Ohio State University, University of Pittsburgh, University of Portsmouth, Princeton University, the United States Naval Observatory, and the University of Washington.

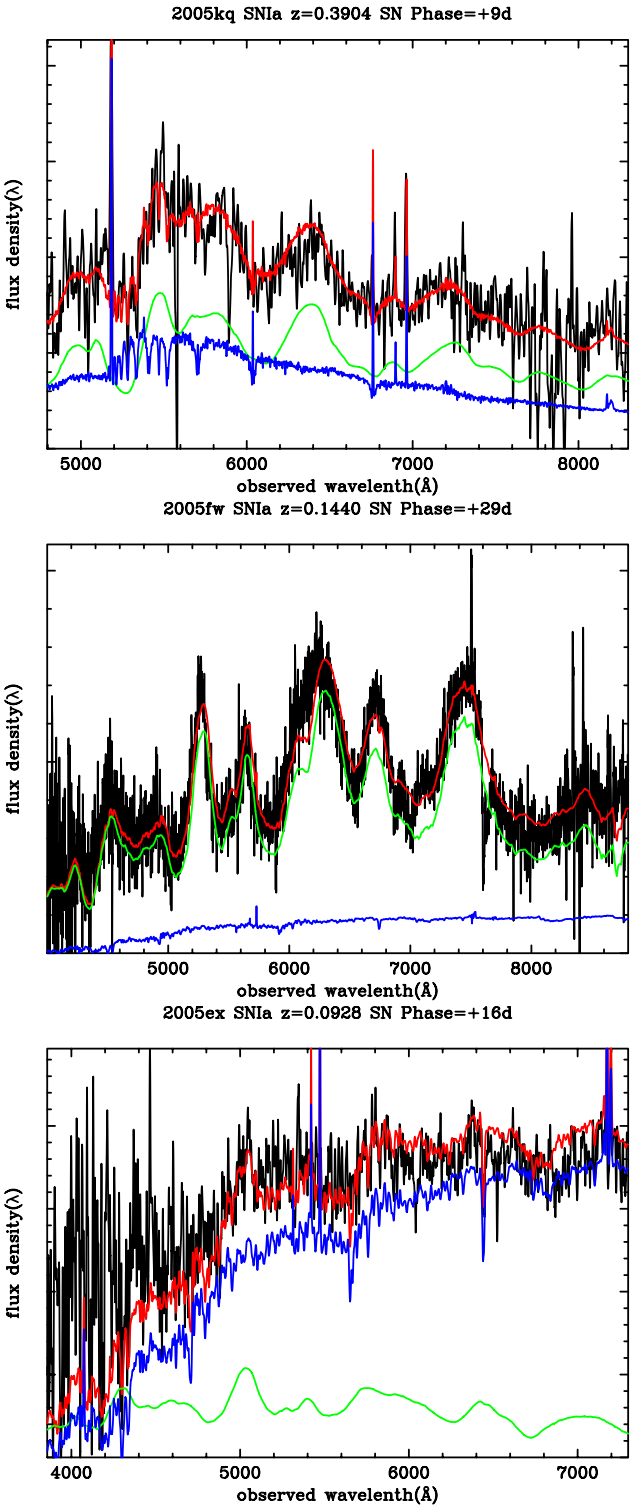

Figure 9. Examples of PCA spectral decomposition. The data (black) are overplotted with the best-fitted combined model (red), with host-galaxy (blue) and SN (green) components. The header of each figure shows the name, redshift, and phase of the SN. The wavelength is shown in the observed frame. The HET spectrum (upper left, resolution: 20 Å) has almost an equal amount of SN and host light. The Subaru spectrum (middle left, resolution: 8–12 Å) has little host contamination, while the MDM spectrum (bottom left, resolution: 15 Å) is dominated by the host.

(A color version of this figure is available in the online journal)

This work is based in part on observations made at the following telescopes. The HET is a joint project of the University of Texas at Austin, the Pennsylvania State University, Stanford University, Ludwig-Maximillians-Universität München, and Georg-August-Universität Göttingen. The HET is named in honor of its principal benefactors, William P. Hobby and Robert E. Eberly. The Marcario Low-Resolution Spectrograph is named for Mike Marcario of High Lonesome Optics, who fabricated several optical elements for the instrument but died before its completion; it is a joint project of the HST partnership and the Instituto de Astronom de la Universidad Nacional Autonoma de Mexico. We thank the HET resident astronomers (John Caldwell, Heinz Edelmann, Steve Odewahn, and Matthew Shetrone) for their continued effort and support with the HET observations. The APO 3.5 m telescope is owned and operated by the ARC. We thank the observatory director, Suzanne Hawley, and site manager, Bruce Gillespie, for their support of this project. The Subaru Telescope is operated by the National Astronomical Observatory of Japan. The William Herschel Telescope is operated by the Isaac Newton Group, and the Nordic Optical Telescope is operated jointly by Denmark, Finland, Iceland, Norway, and Sweden, both on the island of La Palma in the Spanish Observatorio del Roque de los Muchachos of the Instituto de Astrofisica de Canarias. Observations at the ESO New Technology Telescope at La Silla Observatory were made under programme IDs 77.A-0437, 78.A-0325, and 79.A-0715. Kitt Peak National Observatory, National Optical Astronomy Observatories (NOAO), is operated by the Association of Universities for Research in Astronomy, Inc. (AURA) under cooperative agreement with the NSF. The WIYN Observatory is a joint facility of the University of Wisconsin-Madison, Indiana University, Yale University, and NOAO. The W. M. Keck Observatory is operated as a scientific partnership among the California Institute of Technology, the University of California, and NASA. The Observatory was made possible by the generous financial support of the W. M. Keck Foundation. The South African Large Telescope of the South African Astronomical Observatory is operated by a partnership between the National Research Foundation of South Africa, Nicolaus Copernicus Astronomical Center of the Polish Academy of Sciences, the Hobby–Eberly Telescope Board, Rutgers University, Georg-August-Universität Göttingen, University of Wisconsin-Madison, University of Canterbury, University of North Carolina-Chapel Hill, Dartmouth College, Carnegie Mellon University, and the United Kingdom SALT consortium. A.V.F.'s supernova group at U.C. Berkeley is supported by NSF grant AST-0607485.

This work is also supported in part by the U.S. Department of Energy under contract number DE-AC0276SF00515.

REFERENCES

Adelman-McCarthy, J., et al. 2007, ApJS, 172, 634
Aldering, G., et al. 2006, ApJ, 650, 510
Altavilla, G., et al. 2004, MNRAS, 349, 1344
Astier, P., et al. 2006, A&A, 447, 31
Balland, C., et al. 2006, A&A, 445, 387
Benetti, S., et al. 2005, ApJ, 623, 1011
Blondin, S., & Tonry, J. 2007a, AIPC, 924, 312
Blondin, S., & Tonry, J. L. 2007b, ApJ, 666, 1024
Blondin, S., Walsh, J. R., Leibundgut, B., & Sainton, G. 2005, A&A, 431, 757
Branch, D., Fisher, A., & Nugent, P. 1993, AJ, 106, 2383
Branch, D., & Tammann, G. A. 1992, ARA&A, 30, 359
Branch, D., et al. 2002, ApJ, 566, 1005
Cardeli, J. A., Calyton, G. C., & Mathis, J. S. 1989, ApJ, 345, 245
Chornock, R., Filippenko, A. V., Branch, D., Foley, R. J., Jha, S., & Li, W. 2006, PASP, 118, 722
Clocchiatti, A., et al. 1996, ApJ, 462, 462
Connolly, A. J, Szalay, A. S., Bershady, M. A., Kinney, A. L., & Calzetti, D. 1995, AJ, 110, 1071
Copin, Y., et al. 2006, New A Rev., 50, Issue 4-5, 436
Dilday, B., et al. 2008, ApJ, at press (arXiv:0801.3297)
Elmhamdi, A., Danziger, I. J., Cappellaro, E., Della Valle, M., Gouiffes, C., Phillips, M. M., & Turatto, M. 2004, A&A, 426, 963
Ferdinando, P., et al. 2001, ApJ, 555, 900
Filippenko, A. V. 1982, PASP, 94, 715
Filippenko, A. V. 1997, ARA&A, 35, 309
Filippenko, A. V. 2005a, in The Fate of the Most Massive Stars, ed. R. Humphreys, & K. Stanek (San Francisco, CA: ASP), 33
Filippenko, A. V. 2005b, in White Dwarfs: Cosmological and Galactic Probes, ed. E. M. Sion, S. Vennes, & H. L. Shipman (Dordrecht: Springer), 97
Filippenko, A. V., Li, W. D., Treffers, P. R., & Modjaz, M. 2001, PASP, 246, 121
Filippenko, A. V., et al. 1992a, ApJ, 384, L15
Filippenko, A. V., et al. 1992b, AJ, 104, 1543
Foley, R. J., et al. 2003, PASP, 115, 1220
Folkes, S., Lahav, O., & Maddox, S. 1996, MNRAS, 283, 651
Frieman, J. A., et al. 2008, AJ, 135, 238
Fukugita, M., Ichikawa, T., Gunn, J. E., Doi, M., Shimasaku, K., & Schneider, D. P. 1996, AJ, 111, 174
Gal-Yam, A., Ofek, E., & Suemmer, O. 2002, MNRAS, 332, L73
Garavini, G., et al. 2004, AJ, 128, 387
Garnavich, P., et al. 2004, ApJ, 613, 1120
Gunn, J. E., et al. 1998, AJ, 116, 3040
Gunn, J. E., et al. 2006, AJ, 131, 2332
Hamuy, M., et al. 1996, AJ, 112, 2398
Hamuy, M., et al. 2002, AJ, 124, 417
Hamuy, M., et al. 2003, Nature, 424, 651
Hamuy, M., et al. 2006, PASP, 118, 2
Hill, G. J., et al. 1998, Proc. SPIE, 3355, 375
Hook, I., et al. 2005, AJ, 130, 2788
Howell, D. A., & Wang, L. 2002, BAAS, 34, 1256
Howell, D. A., et al. 2005, ApJ, 634, 1190
Hsiao, E. Y., et al. 2007, ApJ, 663, 1187
Ivezic, Z., et al. 2007, AJ, 134, 973
Jha, S., Riess, A. G., & Kirshner, R. P. 2007, ApJ, 659, 122
Jha, S., et al. 1999, ApJS, 125, 73
Jha, S., et al. 2006, AJ, 131, 527
Knop, R. A., et al. 2003, ApJ, 598, 102
Krisciunas, K., et al. 2006, AJ, 131, 1639
Leonard, D. C., et al. 2002, PASP, 114, 35
Li, W. D., et al. 2000, in Cosmic Explosions, ed. S. S. Holt, & W. W. Zhang (New York: AIP), 103
Lidman, C., et al. 2005, A&A, 430, 843
Madgwick, D. S., Hewett, P. C., Mortlock, D. J., & Wang, L. 2003, ApJ, 599, L33
Madgwick, D. S., et al. 2002, MNRAS, 333, 133
Matheson, T., et al. 2001, ApJ, 121, 1648
Matheson, T., et al. 2003, ApJ, 599, 394
Matheson, T., et al. 2005, AJ, 129, 2352
Miknaitis, G., et al. 2007, ApJ, 666, 674
Nugent, P., Kim, A., & Perlmutter, S. 2002, PASP, 114, 803
Oke, J. B., et al. 1995, PASP, 107, 375
Perlmutter, S., et al. 1999, ApJ, 517, 565
Phillips, M. M. 1993, ApJ, 413, L105
Phillips, M. M., et al. 2007, PASP, 119, 360
Prieto, J. L., et al. 2007, AJ, submitted (arXiv:0706.4088)
Pun, C. S. J., et al. 1995, ApJ, 99, 223
Quimby, R., Höflich, P., & Wheeler, J. C. 2007, ApJ, 666, 1083
Riess, A. G. 1996, Ph.D. thesis, Harvard Univ.
Riess, A. G., Press, W. H., & Kirshner, R. P. 1995, ApJ, 438, L17
Riess, A. G., et al. 1998, AJ, 116, 1009
Riess, A. G., et al. 1999, AJ, 117, 707
Riess, A. G., et al. 2004, AJ, 607, 665
Sako, M., et al. 2008, AJ, 135, 348
Shetrone, M., et al. 2007, PASP, 119, 556
Stanek, K. Z., et al. 2003, ApJ, 591, 17
Stathakis, R., et al. 2000, MNRAS, 314, 807
Tonry, J., & Davis, M. 1979, AJ, 84, 10
Turatto, M., Benetti, S., Cappellaro, E., Danziger, I. J., Della Valle, M., Gouiffes, C., Mazzali, P. A., & Patat, F. 1996, MNRAS, 283, 1
Wood-Vasey, W. M., et al. 2007, ApJ, 666, 694
Yip, C. W., et al. 2004, AJ, 128, 585
York, D. G., et al. 2000, AJ, 120, 1579